Modification of cyanobacterial strains for optimised light harvesting and growth in photobioreactors

By Fred Spackman

2021

Abstract

The cyanobacterium *Synechocystis* sp. PCC 6803 (*Synechocystis*) has great potential for industrial biomass and chemical production, but commercialisation is dependent on improving productivity. Cyanobacterial light harvesting is not optimal for growth in photobioreactors and could potentially be improved via genetic modification including: 1) truncation of the phycobilisome, the light harvesting complex, in order to increase light penetration in dense cultures and reduce photoinhibition; 2) Expression of proteorhodopsin, a foreign light harvesting complex, to the thylakoid membrane in order to allow utilisation of green light and increase the spectrum harvested. In order to test the latter hypothesis, a necessary control strain was generated for characterisation of PsaF$_{TS}$PR, a *Synechocystis* strain producing thylakoid membrane targeted proteorhodopsin. Preliminary growth characterisation suggests that PsaF$_{TS}$PR reaches higher cell densities than wild-type when it is grown in cultures that are deep, dense, and not carbon-limited. In order to generate a *Synechocystis* strain with optimal light harvesting properties, a proteorhodopsin gene with a thylakoid membrane targeting sequence was inserted into the chromosomal DNA, replacing a varying number of phycobilisome antenna genes. These mutants were characterized via absorption spectroscopy and oxygen evolution experiments. Absorption spectroscopy concluded that the mutants were not absorbing considerably more green light. This may have been due to low levels of retinal, the chromophore in proteorhodopsin, during exponential phase. Using an oxygen electrode, it was found that the proteorhodopsin expressing strain with a 75% reduced phycobilisome, Olive: PsaF$_{TS}$PR, demonstrated a significantly increased maximum photosynthetic rate of 33.2% compared to wild-type, and 45.4% compared to a strain with only the 75% reduced phycobilisome. This suggests that expression of proteorhodopsin may compensate for the deleterious effects of phycobilisome truncation, specifically the excess capacity for protein production. However, further experiments are required to test whether expression of proteorhodopsin had a role in improving photosynthesis in this strain.

Table of Contents

1 Introduction

1.1 Cyanobacteria

Cyanobacteria, often called “blue-green algae”, are a phylum of Gram-negative bacteria of immense biological importance (Stanier and Bazine, 1977). Cyanobacteria were the first oxygen-evolving organisms and were responsible for the oxygenation of the atmosphere approximately 2.4 billion years ago, a process of monumental consequence (Schopf, 2013). These are both unicellular and multicellular and generally exist anywhere there is water, oceans, hot springs, polar environments, soil or even temporarily moistened rocks in deserts (Waterbury, 2006). They are particularly dominant in the ocean, where they are responsible for approximately half of oceanic oxygen production (Zwirglmaier *et al.*, 2008) and a large proportion of nitrogen fixation (Galloway *et al.*, 2004). The industrial importance, and moreover potential, of cyanobacteria is the focus of this thesis and is discussed in section 1.4.

1.2 *Synechocystis* sp. PCC 6803

Synechocystis sp. PCC 6803 (*Synechocystis*) is a unicellular, freshwater cyanobacteria (Williams, 1988). Characteristic of cyanobacterial species, *Synechocystis* has three membrane systems: an outer membrane, a plasma membrane (PM), and a series of internal thylakoid membranes (TMs) which house the photosynthetic components and separates lumenal spaces from the cytoplasm (Peschek, 1999) (Figure 1). The cytoplasm contains several bodies including the nucleoid (which contains approximately 12 copies of the single chromosome (Labarre, Chauvat and Thuriaux, 1989)), carboxysomes, a carbon fixing compartment, and polyhydroxybutyrate (PHB) granules.

Synechocystis is the most studied model cyanobacterium due to its genetic amenability and ability to grow both autotrophically and heterotrophically on glucose. This allows for the construction of mutants lacking certain photosynthetic components and provides insights into its physiology and biochemistry.

The genome of *Synechocystis* has been sequenced (Kaneko *et al.*, 1996) and many advanced tools have been developed for its genetic manipulation. One such tool is the generation of unmarked mutants, which contain no foreign DNA except when desirable (Lea-Smith, Vasudevan and Howe, 2016). Chromosomal alterations are introduced into a strain via insertion of an antibiotic resistance cassette to generate a marked mutant. The cassette is

subsequently removed using a negative selectable marker. These transformations are carried out using suicide plasmids (plasmids that cannot replicate inside the strain of interest). The plasmids need only be mixed with the cells as *Synechocystis* is naturally competent for DNA uptake (Grigorieva and Shestakov, 1982).

Its history as a model organism makes *Synechocystis* an attractive candidate for industrial cultivation. It can be cultured in fresh or saltwater and requires relatively inexpensive nutrients for growth (Heidorn *et al.*, 2011). A further attribute of the substrain used in the Lea-Smith laboratory is that it cannot readily form biofilms, which are problematic when cyanobacteria are cultured in photobioreactors.

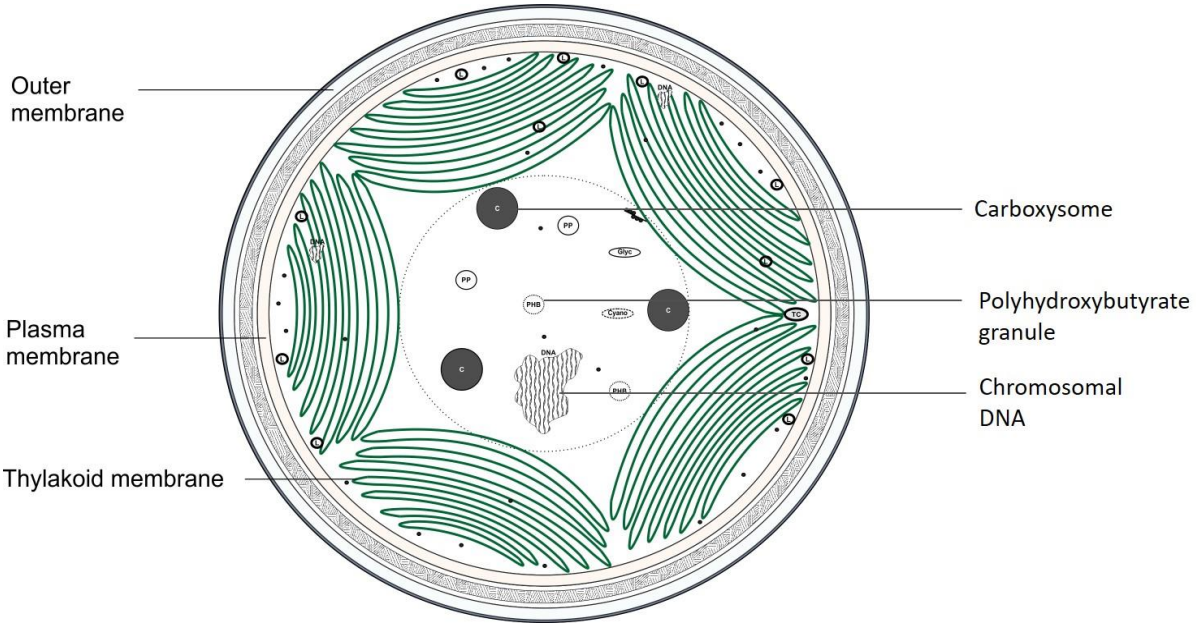

Figure 1. Structure of a *Synechocystis* cell. Modified from Baers *et al.* (Baer *et al.*, manuscript in preparation).

1.3 Cyanobacterial oxygenic photosynthesis

Oxygenic photosynthesis is the process whereby light energy is converted to chemical energy, which is used to fuel cellular activities. This process is carried out by cyanobacteria and their descendants, the chloroplasts found in plants and algae. This section will describe the photosynthetic components of *Synechocystis*, although this process is similar in most cyanobacteria (Lea-Smith *et al.*, 2016).

Solar energy is absorbed by pigment containing protein complexes in the TM (Figure 2). These include the chlorophyll pigments of photosystems I (PSI) and II (PSII), which absorbs light at two peak wavelengths: 430 and 662 nm, and phycobilisomes (PBSs), large light harvesting complexes (LHCs) which associate with the photosystems. The pigments that constitute these antennae, phycocyanin (PC) and allophycocyanin, absorb light with peaks at 620 and 650 nm, respectively. Because of these qualities, PBSs greatly amplify both the quantity and spectra of light absorbed by the photosystems (Zilinskas and Greenwald, 1986; Mullineaux, 1992). In PSII, the energy is used to split water into oxygen, protons and electrons, the latter being transferred via plastoquinone to the cytochrome *b6f* complex (Cyt *b6f*). An electron is then transferred to PSI via cytochrome *c6* (*c6*) or plastocyanin (Pc), where it replaces a newly energized electron. This is transferred to ferredoxin (Fd), then ferredoxin NADPH oxidoreductase (FNR) which uses it to reduce NADP+ to NADPH (Lea-Smith *et al.*, 2016). As the electrons flow linearly, protons are pumped across the TM into the lumen, generating a proton gradient which can be utilized by ATP synthase to produce ATP. NADPH and ATP are energy sources for biological processes, predominantly carbon fixation (McFadden and Tu, 1967).

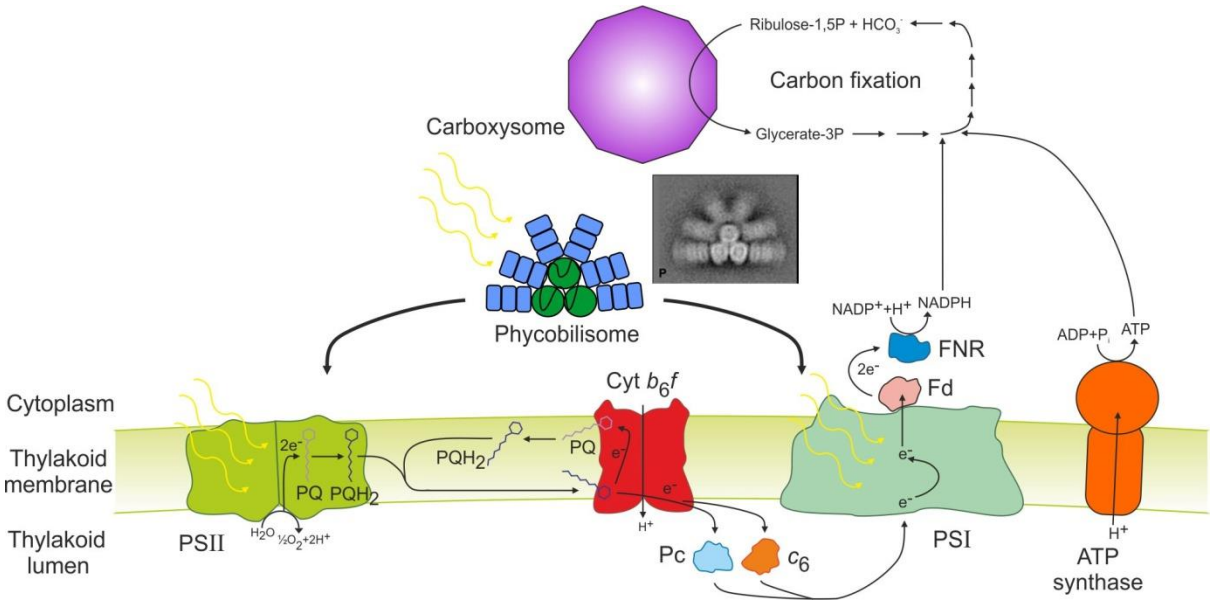

Figure 2. Components involved in the light and dark reactions of cyanobacterial photosynthesis. Lea-Smith *et al.* (Lea-Smith *et al.*, 2016).

1.4 Cyanobacteria as chassis for production of biochemicals

Cyanobacteria may hold significant potential as industrial platforms to produce an array of high and low value biochemicals (Al-Haj *et al.*, 2016). They may be particularly useful for producing plant secondary metabolites, since many processes are conserved between the two groups. Many plant secondary metabolites have beneficial human health effects, such as anticancer, antioxidant, anti-virus, and anti-inflammatory agents, and are difficult to produce in standard biotechnology platforms (Xue and He, 2015). Cyanobacteria, compared to plants, are inherently more efficient at converting solar energy into biomass and do not require arable land (Dismukes *et al.*, 2008). For industrial applications, cyanobacteria are grown in large chambers called photobioreactors, or in raceway ponds. The greatest industrial success of cyanobacteria is the production of high value compounds using *Athrospira plantensis* which is cultivated to produce Spirulina, a nutritious and popular dietary supplement (Kulshreshtha *et al.*, 2008). From such cultures, pure PBS can be isolated and sold as a blue dye (Mary Leema *et al.*, 2010).

Through metabolic engineering and synthetic biology, cyanobacterial strains can be constructed to convert CO_2 directly into commodity chemicals, biofuels, or a precursor of bioplastic (Keasling, 2010; Ducat, Way and Silver, 2011; Wijffels, Kruse and Hellingwerf, 2013). Attempts to mass cultivate recombinant cyanobacteria to produce low value biochemicals, primarily biofuels, has had very limited success, and have also failed to report the reason behind their shortcomings (Lea-Smith and Howe, 2017). Up-scaling efforts are often compromised by contamination, either with competing photosynthetic organisms or predatory ciliates (Wang *et al.*, 2013; Fulbright *et al.*, 2018). Also, genetic instability of the engineered strains may be an issue (Cassier-Chauvat, Veaudor and Chauvat, 2016). However, the prevalent reason is high production costs. Analyses has shown microalgae-derived biofuels to be seven-fold more expensive than the cost required for commercial viability, predominately due to capital and labor costs (Tredici *et al.*, 2016). There are also considerable energy costs involved in agitation of cultures and processing of biomass, dewatering being a major factor (Hoffman *et al.*, 2017; Fasaei *et al.*, 2018). High energy requirements also deduct from environmental sustainability.

There are several improvements which could make the cultivation of cyanobacteria for low value chemicals and biofuel economically feasible (Perin and Jones, 2019). These include optimisation of industrial processes, uncoupling of synthesis and biomass production (which

would likely involve genetically engineering cyanobacteria to secrete target molecules) and enhancement of cyanobacteria's photosynthetic efficiency to increase biomass yield. Improving the latter is the focus of this work.

1.4 Attenuation of the cyanobacterial light harvesting complex

PBSs allow cyanobacterial cells to survive in low light (Kehoe, 2010) and provide a competitive edge by restricting the amount of light absorbed by other cells in the environment (Kirst, Formighieri and Melis, 2014). However, this excessive absorption of photons is not optimal for industrial growth (Melis, 2009). In a photobioreactor, most of the light is absorbed by cells at the surface (typically >90% in the first cm) (Lea-Smith *et al.*, 2014). Since these cells absorb far more energy than is required for photosynthesis, the excess is wasted as heat or fluorescence. It also results in increased photoinhibition (damage of PSII) and production of reactive oxygen species, which further damage the cells (Mussgnug *et al.*, 2007). The Truncated Light-Harvesting Antennae (TLA) concept is that reducing the amount of light absorbed per cell, via LHC reduction, will allow light to penetrate deeper into a culture where photosynthesis is light-limited, whilst reducing photoinhibition and energy waste in surface cells. This theory has been implemented in both cyanobacteria and green algae. In the green alga *Chlamydomonas reinhardtii*, there is evidence that LHC reduction has a positive effect on whole culture productivity (Polle, Kanakagiri and Melis, 2003; Mussgnug *et al.*, 2007; Beckmann *et al.*, 2009; Melis, 2009; Kosourov, Ghirardi and Seibert, 2011).

The PBS of *Synechocystis* consists of a core of three cylinders containing allophycocyanin and six rods radiating from this core, each containing three stacked hexamers of PC (Figure 3). Each PC consists of an α and β subunit, encoded by *cpcA* and *cpcB*, respectively (Plank and Anderson, 1995). The PC hexamers are connected by linker proteins (Zilinskas and Greenwald, 1986). The hexamer distal to the core is connected by CpcC1, the middle hexamer by CpcC2 (Ughy and Ajlani, 2004) and the proximal hexamer by CpcG1 or CpcG2 (Kondo *et al.*, 2007). The distal ends of the rods are also capped by CpcD.

Several studies have reduced the PBS by deletion of the genes for the PC α and β subunits (*cpcA* and *cpcB*) and the linker proteins (*cpcC1* and *cpcC2*), generating an Olive strain, named after the resultant hue. Experiments have been conducted to study the strains' growth and oxygen evolution which can assess the strains' photosynthetic efficiency.

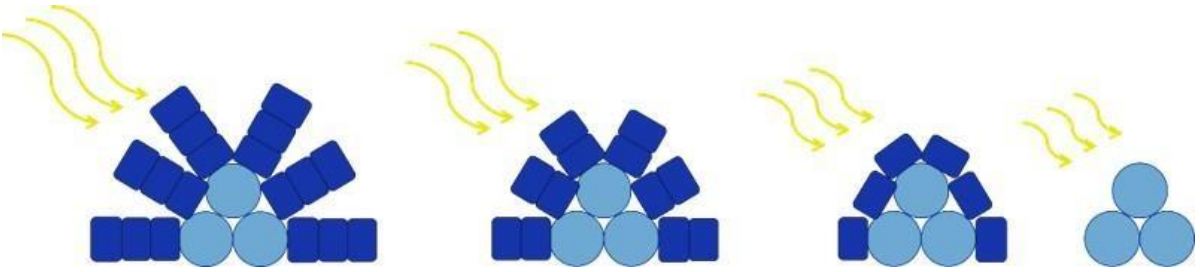

Figure 3. A gradual depletion of the phycobilosomes PC rods (dark blue) and the subsequent decrease in light absorption. From left to right: wild-type, ΔCpcC2: p_{cpc}T->C, ΔCpcC1C2: p_{cpc}T->C, Olive. Allophycocyanin cylinders shown in light blue.

Lea-Smith *et al*. (Lea-Smith *et al.*, 2014) studied an unmarked Olive strain. Growth of this strain was studied in reactors of 10 cm pathlength. The strain exhibited reduced growth under moderate light intensities (40 and 150 µmol photons m^{-2} s^{-1}) and similar growth under high light intensity (500 µmol photons m^{-2} s^{-1}) with CO_2 sparging. However, the strain exhibited significantly reduced levels of photoinhibition under 1000 and 2000 µmol photons m^{-2} s^{-1}. Lea-Smith *et al.* also generated strains with partial phycobilisome truncations (Figure 3), lacking one PC per rod (ΔCpcC1C2: p_{cpc}T->C) and two PC per rod (ΔCpcC1C2: p_{cpc}T->C). In these mutants, the *cpcB* promoter was altered to reduce its strength (Imashimizu *et al.*, 2003) – which effectively removed PBS disassociated PC that was produced from removal of just the linker proteins. These strains exhibited a similar, yet less pronounced, phenotype to Olive.

The Olive strain, generated by Lea-Smith *et al*. (Lea-Smith *et al.*, 2014) also exhibited a large reduction in its maximum oxygen evolution compared to wild-type, suggesting that individual cells had a decreased maximum photosynthetic efficiency, and it exhibited a reduction in cell size. This could be attributed to an excess capacity in the cell for protein production, resulting in an increase in expression of a broad range of genes (Liberton *et al.*, 2017). This is because a large portion of soluble protein in *Synechocystis* cells is composed of PBS subunits (Kwon *et al.*, 2013).

Page *et al*. (Page, Liberton and Pakrasi, 2012) studied a marked Olive knockout, in which *cpcBAC1C2* had been replaced by a cassette containing a Kanamycin resistance gene and a sucrose sensitivity gene, generated by Ughy and Ajlani (Ughy and Ajlani, unpublished work). Under moderate light intensities (50 and 150 µmol photons m^{-2} s^{-1}) and in a photobioreactor with a path length of 2 cm, the Olive strain showed reduced growth compared to wild-type. At

these path lengths any productivity benefits due to greater light penetration would not be observed (Ritchie and Larkum, 2012).

Kirst *et al*. (Kirst, Formighieri and Melis, 2014) studied a different marked Olive strain, in which *cpcBAC1C2D* had been replaced by a Kanamycin resistance cassette. Growth was studied in a large reactor with a 14 cm pathlength and with CO_2 bubbling, so that carbon would not be limited. Under moderate light intensities (50 and 170 µmol photons m^{-2} s^{-1}) Olive exhibited slightly reduced growth, but under high light intensity (2000 µmol photons m^{-2} s^{-1}) Olive showed a significantly increased growth rate. This suggests that the productivity of the culture is improved because of increased light penetration.

Study into the size of Olive cells, by Kirst *et al.*, found no significant difference from wild-type. It may be that the expression of a resistance marker reduces the excess capacity in the cell for protein production, observed by Lea Smith *et al*. Kirst *et al.* also found that the maximum oxygen evolution rate was similar to wild-type's. However, a greater light intensity was required to reach this rate.

Nakajima and Ueda (Nakajima and Ueda, 1997) studied a strain in which PC expression had been reduced by 70%. In this strain cell size was also significantly reduced. Results from oxygen evolution experiments showed that maximum oxygen evolution was similar to wild-type, but was reached at a higher light intensity, in agreement with Kirst *et al*. However, maximum oxygen evolution was greater than that of wild-type in dense cultures, suggesting that the modification could increases maximum photosynthetic efficiency of whole cultures – but not individual cells.

Collectively, the results of these studies suggest that PBS truncation reduced the ability of individual cells to absorb light. This protects cells from photodamage, resulting from excessive light and limiting CO_2. Furthermore, culture productivity may be increased in cultures of Olive that are either dense or deep, due to increased light penetration, but this has not been conclusively proven.

1.5 Proteorhodopsin expression in cyanobacteria

Productivity of a photosynthetic organism could also potentially be improved by broadening the spectra of light absorbed (Chen and Blankenship, 2011). Cyanobacteria exhibit poor absorption of the green portion of the light spectrum (500-570 nm), which is not utilized by either PSI or PSII, or the PBS (Figure 4). Light is unable to penetrate deep into a dense cyanobacterial culture in photobioreactors and this limits photosynthesis. However, green light can penetrate further. The introduction of a protein that can harvest green light and improve chemical energy production may increase biomass yields.

Rhodopsins are light-responsive transmembrane proteins which bind retinal as a chromophore (Craig and Schlesinger, 1985). Proteorhodopsins (PRs), a family of rhodpsins, are highly abundant in ocean bacterioplankton (Dubinsky *et al.*, 2017) where they utilize light (from the green or blue portion of the light spectrum) for proton pumping (Beja *et al.*, 2000) to increase ATP production (Martinez *et al.*, 2007; Pinhassi *et al.*, 2016). Only one known cyanobacterium, *Gloeobacter violaceus*, utilizes PR. It is also the only strain that lacks TMs (Rexroth *et al.*, 2011). It is hypothesized that PR enhances energy production in this strain, which may be low due to the reduction of chlorophyll-based photosynthesis (Choi *et al.*, 2014). This suggests that PR can work alongside photosynthetic components and contribute to photosynthesis. Incorporation of a green light driven PR could increase the productivity of *Synechocystis* cultures.

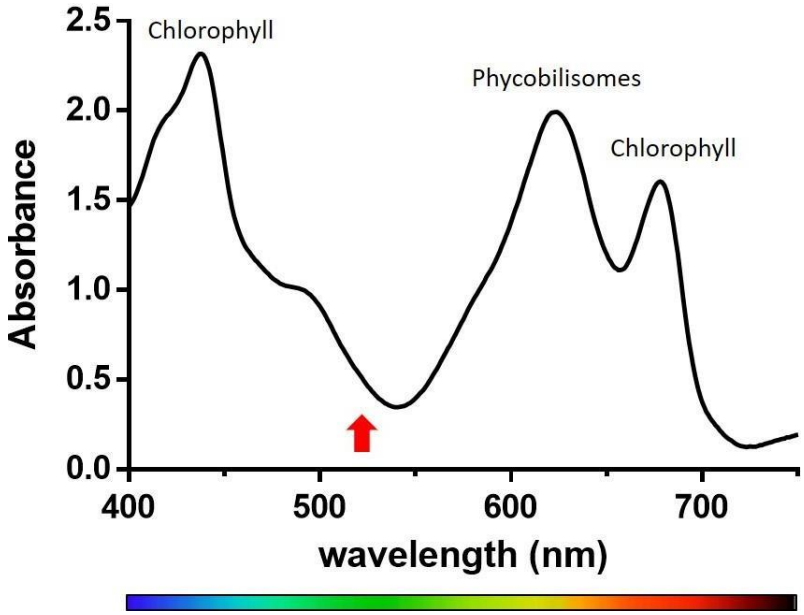

Figure 4. Absorption spectra of *Synechocystis*. Red arrow indicates the λmax of the PR used in this study.

In a study by *Chen et al.*, PR was successfully expressed in *Synechocystis* using a plasmid expression system. This mutant showed marginal increased growth in comparison to a strain expressing a non-functional form of the protein, suggesting that PR is potentially beneficial (Chen *et al.*, 2016). However, growth was not improved in comparison to wild-type, likely due to the metabolic burden of PR expression using a plasmid system – which often results in high and unstable expression (Berla *et al.*, 2013). In a further study by Chen *et al.*, plasmid expression of PR in a photosynthetically impaired background mutant lacking PSI increased growth rate by 30% compared to the non-functional PR copy, under 25 µmol photons m^{-2} s^{-1} of green light. Though, this result is not reliable due to the irregular pattern of the growth (Chen, Arents, *et al.*, 2018). This work also demonstrated that *Synechocystis* expresses retinal and that it will bind to PR, a key prerequisite for a functional protein.

The native form of PR localizes to the TM and the PM (Chen *et al.*, 2016; Baers *et al.*, manuscript in preparation). However, energy absorbance by PM localized PR is not likely to increase ATP production, as the TM is the main site of ATP synthase (Liberton *et al.*, 2016; Baers *et al.*, 2019). Therefore, targeting PR specifically to the TM is likely the best approach to increasing ATP production. Our group previously targeted a PR, which absorbs light at λmax = 520 nm, specifically to the TM in Synechocystis. The PR gene (*PR*) was taken from an uncultured proteobacterium EBAC31A08 (Béjà *et al.*, 2001) and codon optimised for *Synechocystis* (Baers *et al.*, manuscript in preparation). TM targeting was achieved by replacing the native N-terminal targeting sequence of *PR* with that of *psaF*, which encodes a PSI component (PsaF) (Baers *et al.*, manuscript in preparation). This was carried out using an integrative expression vector where the locus *phaAB* was disrupted by *PR* as well as a C-terminal *myc*-tag and a Kanamycin-resistance gene (Figure 5A). The deleted *phaA* and *phaB* genes encode the first two enzymes of the PHB biosynthetic pathway (Korotkova and Lidstrom, 2001). PHB is a storage compound accumulated under stress conditions (Ackermann *et al.*, 1995). This site was chosen because the PHB pathway is non-essential (Stal, 1992) and the site has been used previously for expression cassette integration (Qi *et al.*, 2013). However, this study did not confirm whether growth was affected by the deletion of these genes. The promoter used was that of the *cpc* operon, which provides strong, light induced expression (Liu, Sheng and Curtiss III, 2011).

Also generated in this study were two strains in which PR expresses the Native targeting sequence (NativeTSPR) and that of MscS (MscSTSPR)MscS is a PM localised protein and it

was expected that using this signal sequence would target proteins specifically to this compartment. A method of targeting proteins to the PM would be extremely valuable as a means of targeting proteins to this compartment that could export compounds produced in engineered strains, thus lowering the costs of harvesting. However, both the native and MscS sequence targeted PR indiscriminately to the TM and PM. Protein targeting was confirmed by membrane separation followed by western blot analysis (Figure 5B).

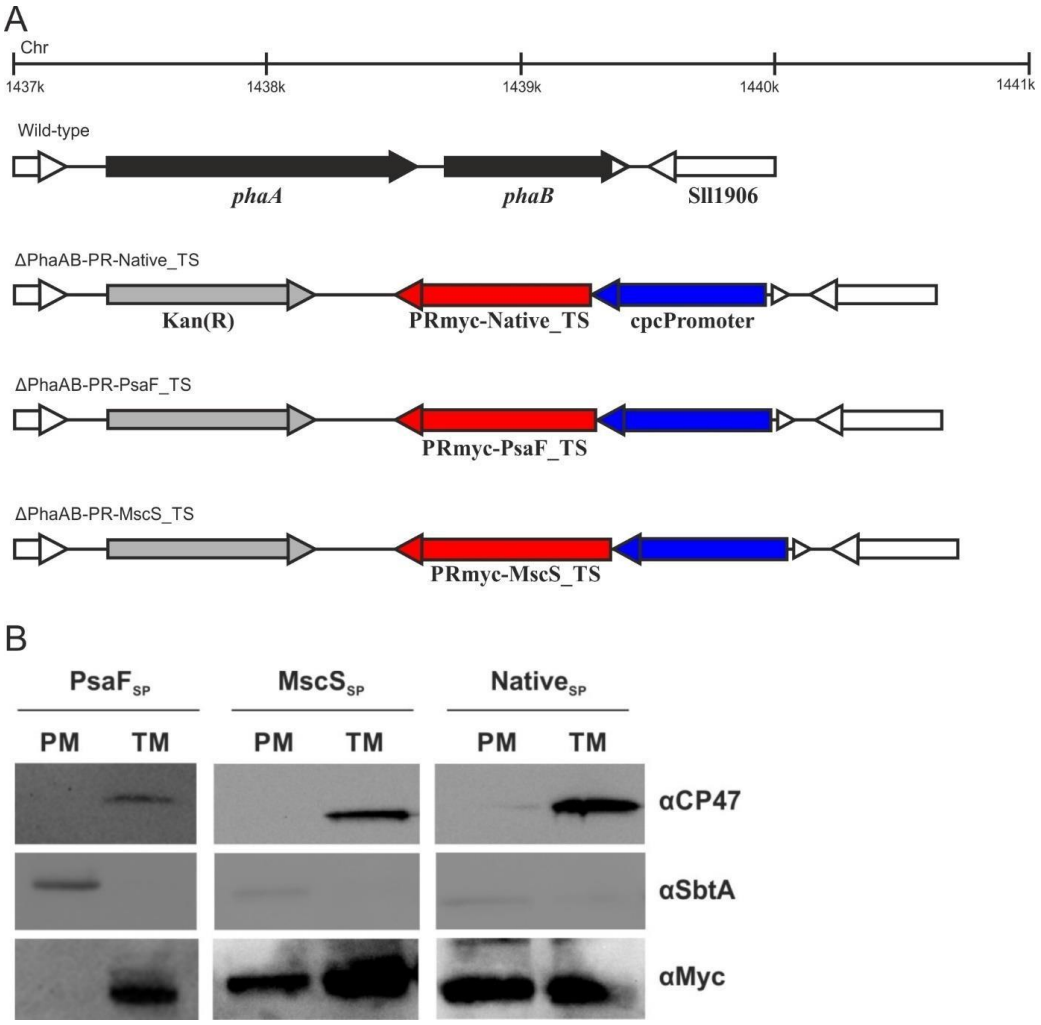

Figure 5. Insertion of PR into the genomic DNA of Synechocystis at the locus phaAB resulted in PR. (a) Genotype of (from top to bottom) wild-type, ΔPhaAB, Native$_{TS}$PR, PsaF$_{TS}$PR and MscS$_{TS}$PR. Scale is the locus location in the *Synechocystis* genome. Regions deleted in the mutant strains are shaded in black, *npt1* is shaded in grey, *PR* is shaded in red and *cpcB* promoter is shaded in blue. **(b)** PR produced in the mutants targeted exclusively to the TM in PsaF$_{TS}$PR, and to the TM and PM in Native$_{TS}$PR and MscS$_{TS}$PR. Western blot analysis to confirm purity of PM and TM samples used antibodies against TM (CP47; 47 kDa) and PM (SbtA; 39 kDa) specific proteins. Localisation of recombinant PR was examined using an anti c-Myc antibody (Baers *et al.*, manuscript in preparation).

The mutant (PsaF$_{TS}$PR) showed an increased growth rate over wild-type *Synechocystis*, which resulted in a 13% increase in cell density, measured by Optical density (OD) at 750 nm, when cells were cultured under continuous light of 100 µmol photons m^{-2} s^{-1} with air bubbling in a 1L photobioreactor. The growth of the strains only diverged during the late logarithmic phase, when OD_{750nm} was above 2 (Figure 6). This difference in growth between PsaF$_{TS}$PR and wild-type was not observed in a photobioreactor with a smaller pathlength (Figure 7D), or under moderate white light (50 µmol photons m^{-2} s^{-1}) or low white light (5 µmol photons m^{-2} s^{-1}) without air bubbling (Figure 7AB). PsaF$_{TS}$PR did however exhibit improved growth under moderate green light (20 µmol photons m^{-2} s^{-1}) without air bubbling (Figure 7C). Green light was used in order to dampen the activity of photosystems and the PBS in contrast to PR.

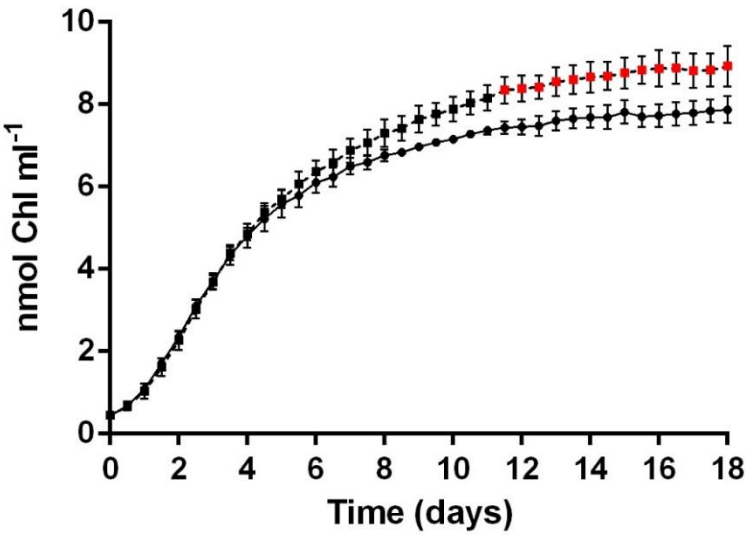

Figure 6. PR expression led to increased growth under high light intensity, air bubbling and increased pathlength. Growth of wild-type (circles) and PsaF$_{TS}$PR (squares) under 100 µmol photons m^{-2} s^{-1} in a 1L conical flask + air bubbling. Pink shapes indicate significant differences between wild-type and PsaF$_{TS}$PR expressing strains ($P<0.05$). Error bars are standard error of three replicates. (Baers *et al.*, manuscript in preparation)

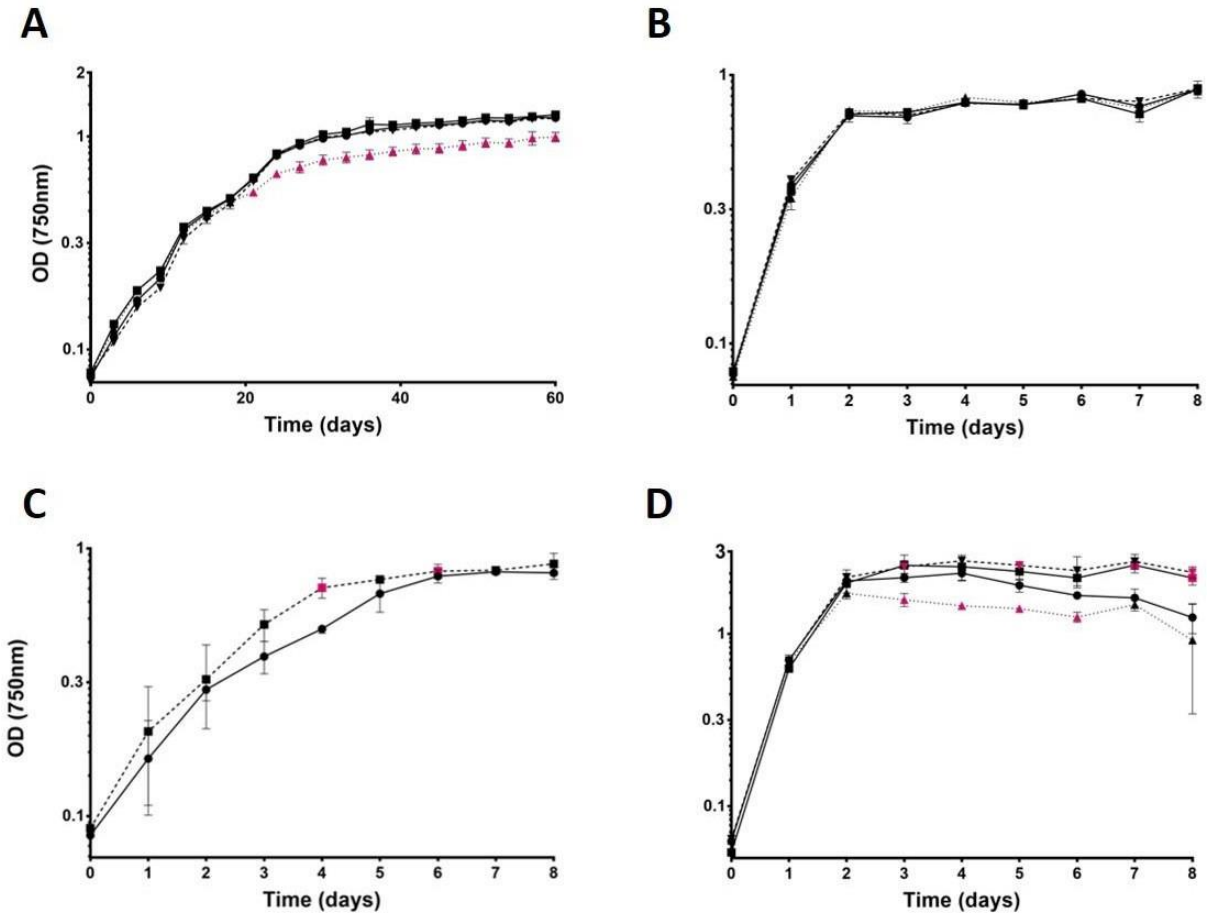

Figure 7. PR expression increased growth under green light during later growth phases. PR expression did not result in increased growth rates under low light intensities. Growth on a Log^{10} scale of cultures grown under: **(a)** 5 µmol photons m^{-2} s^{-1} **(b)** 50 µmol photons m^{-2} s^{-1} **(c)** 50 µmol photons m^{-2} s^{-1} of green light and **(d)** 100 µmol photons m^{-2} s^{-1} + air bubbling. Stains included are wild-type (circles), $Native_{TS}PR$ (upside-down triangles), $PsaF_{TS}PR$ (squares) and $MscS_{TS}PR$ (triangles). Errors bars are standard deviation. Red highlighting indicates statistical difference. (Baers *et al.*, manuscript in preparation).

2 Aims

This study has two aims.

1. To assess whether deletion of the *phaAB* genes and not the introduction of PR to the TM of *Synechocystis* was responsible for the increased biomass accumulation observed in the PsaF$_{TS}$PR strain. This will require construction of an unmarked *phaAB* knockout strain, the growth of which will be compared to PsaF$_{TS}$PR under the conditions shown most promising in previous characterisation.

2. To generate and test a *PR* expressing, PBS attenuated mutant with optimal light harvesting properties for conditions similar to those used in industrial photobioreactors. *PR* will be inserted into the *cpc* operon, replacing the genes encoding the PC portion of the PBS. *PR* expression and PBS truncation may both be apt methods of optimizing *Synechocystis*' light absorption properties for growth in photobioreactors. The former increasing the spectra of light absorbed by cells, and the latter increasing light penetration and reducing photoinhibition. Furthermore, *PR* expression should counteract the negative phenotype which results from cellular protein reduction contributed to PBS truncation.

3 Materials and methods

3.1 Generation of a PhaAB unmarked knockout

Plasmids used and constructed in this study are listed in Table 1. Primers used in this study are listed in Table 2. PCR was performed by standard procedures using Phusion high- fidelity DNA polymerase (NEB). Generation of an unmarked mutant, from a marked *phaAB* knockout strain, was carried out according to Xu *et al.* (Xu *et al.*, 2004). To remove the *npt1*/*sacRB* cassette, the strain was transformed with 1 µg of the markerless pPhaAB-UM construct. Following incubation in BG-11 liquid medium for 4 days and agar plates containing sucrose for a further 1 to 2 weeks, transformants were patched on kanamycin and sucrose plates. Sucrose-resistant, Kanamycin-sensitive ΔPhaAB containing the unmarked deletion were confirmed by PCR using primers flanking the deleted region.

Table 1. Plasmids used/constructed in this study.

Plasmid name	Flanking regions	ORF	Reference
pCpcC2-1	*cpcC2*	Not applicable	Lea-Smith *et al.*, 2014
pCpcC1C2-1	*cpcC1C2*	Not applicable	Lea-Smith *et al.*, 2014
pCpcBAC1C2-1	*cpcBAC1C2*	Not applicable	Lea-Smith *et al.*, 2014
pCpcC2-2	*cpcC2*	*sacRB*/ *npt1*	Lea-Smith *et al.*, 2014
pPhaAB-UM	*phaAB*	Not applicable	Baers *et al.*, manuscript in preparation
pPR-Myc	*phaAB*	*cpcB* promoter/ PsaF targeting sequence/ *PR*/ *myc*-tag/ *npt1*	Baers *et al.*, manuscript in preparation
pCpcC2-PR	*cpcC2*	PsaF targeting sequence/ *PR*	This study
pCpcC2-PR-Myc	*cpcC2*	PsaF targeting sequence/ *PR*/ *myc*-tag	This study
pCpcC1C2-PR	*cpcC1C2*	PsaF targeting sequence/ proteorhodopsin	This study
pCpcC1C2-PR-Myc	*cpcC1C2*	PsaF targeting sequence/ *PR*	This study
pCpcBAC1C2- PR	*cpcBAC1C2*	PsaF targeting sequence/ *PR*	This study
pCpcBAC1C2-PR-Myc	*cpcBAC1C2*	PsaF targeting sequence/ *PR*	This study

ORF: Open reading frame to be expressed

Table 2. Sequence of primers used in this study.

Primer name	Sequence (5' to 3')
CpcC2PRfor	GACACTTATCTAGGAGAACAAAATGAAACATTTGTTGGCGTTGCTCCT
CpcC2PRrev+myc	GTTGACAAAAAATCCTGATTCTAATTCAGATCCTCTTCTGAGATG
CpcC2PRrev	GTTGACAAAAAATCCTGATTCTAGGCATTGGAGGATTCTTTCACGGC
CpcC1C2PRrev+myc	CTCCTGAACTAAACAGAAATCTAATTCAGATCCTCTTCTGAGATG
CpcC1C2Prrev	CTCCTGAACTAAACAGAAATCTAGGCATTGGAGGATTCTTTCACGGC
CpcopePRfor	GTCAAGTAGGAGATTAATTCAATGAAACATTTGTTGGCGTTGCTCCT
PRforCpcC2	GCAACGCCAACAAATGTTTCATTTTGTTCTCCTAGATAAGTG
PRrev+mycCpcC2	CTCATCTCAGAAGAGGATCTGAATTAGAATCAGGATTTTTTGTCAA
PRrevCpcC2	GCCGTGAAAGAATCCTCCAATGCCTAGAATCAGGATTTTTTGTCAA
PRrev+mycCpcC1C2	CTCATCTCAGAAGAGGATCTGAATTAGATTTCTGTTTAGTTCAGGAG
PRrevCpcC1C2	GCCGTGAAAGAATCCTCCAATGCCTAGATTTCTGTTTAGTTCAGGAG
PRforCpcope	GCAACGCCAACAAATGTTTCATTGAATTAATCTCCTACTTG
PhaABfor	GTGCGGAATTTCAGGACAA
PhaABrev	GTGGTGGCTCGCTTTGAC
cpcC2for	AAAGTCAGGGCGTAACTCCA
cpcC2rev	CCGCTTTTCCAGGTCTTGTC
cpcC1C2for	GTTTTCATTGGCATCGGTCT
cpcOPErev	GGTTGTCTTCCCTTCCCAAT
PRcheckfor	GACCGTGCCCTTGTTGATTT
PRcheckrev	CTTTCACGGCCACATTCCAA

3.2 Plasmid construction

The genome sequence of *Synechocystis* (Kaneko *et al.*, 1996) was consulted via CyanoBase (http://genome.microbedb.jp/cyanobase/GCA_001318385.1) for primer design. Plasmids for the unmarked replacement of phycobilisome genes with *PR* were constructed via Gibson cloning. Plasmid vectors were produced from PBS truncation plasmids: pCpcC2-1, pCpcC1C2-1, and pCpcBAC1C2-1. *PR*, with or without a *Myc*-tag, was taken from pPhaAB-PR-Myc. The primed vectors and *PR* inserts were verified via gel electrophoresis. Corresponding inserts and vectors were assembled using Gibson Assembly® Master Mix (NEB) according to the manufacturer's protocol. This inserted PR, with or without a Myc tag, between the flanking regions of the PBS truncation plasmids, seamlessly in between the start codon of one PBS gene and the stop codon of another PBS gene. The 6 resulting plasmids: pCpcC2-PR, pCpcC2-PR-Myc, pCpcC1C2-PR, pCpcC1C2-PR-Myc, pCpcBAC1C2-PR and pCpcBAC1C2-PR-Myc, were introduced via heat shock into competent *Escherichia coli* cells. Plasmids were isolated using a QIAprep Spin Miniprep Kit (QIAGEN) according to the manufacturer's protocol. Plasmids were verified by digestion with *Eco*RI and *Bam*HI followed by gel electrophoresis (Figure 20). Further verification was carried out via sequencing.

3.3 Generation of PR expressing TLA strains

Synechocystis strains used and constructed in this study are listed in Table S3. Marked knockouts of ΔCpcC2: p_{cpc}T->C and ΔCpcC1C2: p_{cpc}T->C were produced via introduction of the plasmids pCpcC2-2 and pCpcC1C2-2, respectively, into p_{cpc}T->C. Olive marked knockout was generated via the introduction of pCpcBAC1C2-2 into wild-type. These transformations were carried out following the protocol outlined in Lea-Smith *et al.* (Lea-Smith, Vasudevan and Howe, 2016). Approximately 1 µg of the plasmid was mixed with cells for 6 hours. Cells were then incubated on agar plates for 24 hours before an additional 3 ml of agar containing kanamycin was added to the surface of the plates, followed by further incubation for one to two weeks. Transformants were sub-cultured and confirmed by PCR. *npt1*/*sacRB* cassettes were replaced with *PR* or *PR-myc* cassettes via the following transformations:

- ΔCpcC2: p_{cpc}T->C with pCpcC2-PR to produce ΔCpcC2: p_{cpc}T->C: PsaF_{TS}PR
- ΔCpcC2: p_{cpc}T->C with pCpcC2-PR-Myc to produce ΔCpcC2: p_{cpc}T->C: PsaF_{TS}PR-Myc
- ΔCpcC1C2: p_{cpc}T->C with pCpcC1C2-PR to produce ΔCpcC1C2: p_{cpc}T->C: PsaF_{TS}PR
- ΔCpcC1C2: p_{cpc}T->C with pCpcC1C2-PR-Myc to produce ΔCpcC1C2: p_{cpc}T->C: PsaF_{TS}PR-Myc
- Olive with pCpcBAC1C2-PR to produce Olive: PsaF_{TS}PR
- Olive with pCpcBAC1C2-PR-Myc to produce Olive: PsaF_{TS}PR-Myc

These were carried out following the methodology described in Section 5.1. Strains were verified via PCR assay and sequencing using primers flanking the modified region.

Table S3. Strains used/constructed in this study.

Strain	Genotype	Reference
wild-type	*Synechocystis* sp. PCC 6803 Wild type	Williams *et al.*, 1988
p_{cpc}T->C	Wild type/ T→C 258 upstream of *cpcB* start codon	Lea-Smith *et al.*, 2014
ΔCpcC2: p_{cpc}T->C	Δ*cpcC2*/ T→C 258 upstream of *cpcB* start codon	Lea-Smith *et al.*, 2014
ΔCpcC1C2: p_{cpc}T->C	Δ*cpcC1C2*/ T→C 258 upstream of *cpcB* start codon	Lea-*Smith et al.*, 2014
Olive	Δ*cpcBAC1C2*	Lea-Smith *et al.*, 2014
ΔPhaAB	Δ*phaAB*	This study
$PsaF_{TS}$PR	Δ*phaAB*/ proteorhodopsin gene + targeting sequence from *psaF* (*sll0819*) + *myc*-tag/ *npt1*	Baers *et al.*, manuscript in preparation
$MscS_{TS}$PR	Δ*phaAB*/ proteorhodopsin gene + targeting sequence from *mscS* (*slr0765*) + *myc*-tag/ *npt1*	Baers *et al.*, manuscript in preparation
$Native_{TS}$PR	Δp*haAB*/ proteorhodopsin gene + *myc*-tag/ *npt1*	Baers *et al.*, manuscript in preparation
ΔCpcC2: p_{cpc}T->C: $PsaF_{TS}$PR	ΔCpcC2/ T→C 258 upstream of *cpcB* start codon /proteorhodopsin + targeting sequence from *psaF* (*sll0819*)	This study
ΔCpcC2: p_{cpc}T->C: $PsaF_{TS}$PR-Myc	Δ*cpcC2*/ T→C 258 upstream of *cpcB* start codon/ proteorhodopsin gene + targeting sequence from *psaF* (*sll0819*) + *myc*-tag	This Study
ΔCpcC1C2: p_{cpc}T->C: $PsaF_{TS}$PR	Δ*cpcC1C2*/ T→C 258 upstream of *cpcB* start codon/ proteorhodopsin gene + targeting sequence from *psaF* (*sll0819*)	This study
ΔCpcC1C2: p_{cpc}T->C: $PsaF_{TS}$PR-Myc	Δ*cpcC1C2*/T→C 258 upstream of *cpcB* start codon/ proteorhodopsin gene + targeting sequence from *psaF* (*sll0819*) + *myc*-tag	This study
Olive: $PsaF_{TS}$PR	Δ*cpcBAC1C2*/ proteorhodopsin gene + targeting sequence from *psaF* (*sll0819*)	This study
Olive: $PsaF_{TS}$PR-Myc	Δ*cpcBAC1C2*/ proteorhodopsin gene + targeting sequence from *psaF* (*sll0819*) + *myc*-tag	This study

3.4 Growth conditions

Starter cultures were grown at 30°C under 40 µmol photons m^{-2} s^{-1} of continuous white light and shaking at 200rpm. Air was bubbled to reduce photoinhibition and extend the length of the logarithmic phase. Starter cultures were grown to OD_{750nm} = ~1, which is logarithmic phase under these conditions. To characterize growth under green light, strains were cultured under both moderate continuous green and white light (50 µmol photons m^{-2} s^{-1}). Individual starter cultures were used to inoculate three technical replicates under each condition. Cultures were grown in 12 well plates, in volumes of 3 ml. To characterize growth in larger volume photobioreactors. Strains were cultured under 100 µmol photons m^{-2} s^{-1} of continuous white light with air bubbling and shaking at 150 rpm in volumes of 600 ml in order to increase the path-length. A Student's paired *t*-test was used for all comparisons, $P < 0.05$ being considered statistically significant.

3.5 Analysis of absorption spectra

Absorption profiles of strains was measured according to Hervey *et al.* (Hervey *et al.*, manuscript in preparation). Two quartz cuvettes were used in the dual-beam spectrophotometer. In these customized cuvettes, the chamber is divided into two compartments, each with an optical path of 5 mm. The cuvettes were orientated so that the investigation beam passed through both chambers. A baseline reading was taken with blank growth medium in one chamber of both cuvettes (i.e., the sample and the reference cuvettes) and a 1 mg ml^{-1} suspension of titanium dioxide in water in the other chamber. The titanium dioxide suspension was placed in the chamber closer to the light source, such that the beam passed through the suspension before passing through the sample. The spectrophotometer was zeroed with this setup by recording a baseline correction. To record a spectrum, the titanium dioxide suspension was left in place in both cuvettes, but the blank medium in the sample cuvette was replaced with the sample.

3.6 Measurement of oxygen evolution

Photosynthetic oxygen evolution rates and oxygen depletion rates were determined from cultures of OD_{750nm} = ~0.35 using an oxygen electrode system (Hansatech Ltd) maintained at 30°C. Following dark equilibration (10 min), oxygen exchange rates were recorded for 10 min at increasing light intensities (10, 25, 60, 150, 350 and 900 µmol photons m^{-2} s^{-1}). Each light period was followed immediately by 10 min in darkness to calculate the respiration rates. The respiration rate following illumination at each light intensity was subtracted to estimate the gross rate of photosynthetic oxygen evolution. A Student's paired *t*-test was used for all comparisons, $P < 0.05$ being considered statistically significant.

4 Results

4.1 Generation of an unmarked *phaAB* deletion mutant

In order to confirm whether removal of the PHB pathway affects the growth of $PsaF_{TS}PR$, an unmarked *Synechocystis* mutant lacking *phaAB* was constructed as a control strain for characterisation. The locus was disrupted via a two-step homologous recombination protocol. The strain was constructed from a marked strain, generated previously, in which the *phaAB* locus was disrupted by a cassette encoding *npt1*/ *sacRB*. A markerless construct containing a deleted copy of *phaAB* and lacking the *npt1*/ *sacRB* cassette was introduced, and cells were cultured in the presence of sucrose to select for recombination-mediated removal of the cassette. Complete segregation was confirmed by PCR assay with primers upstream and downstream of the locus (Figure 8).

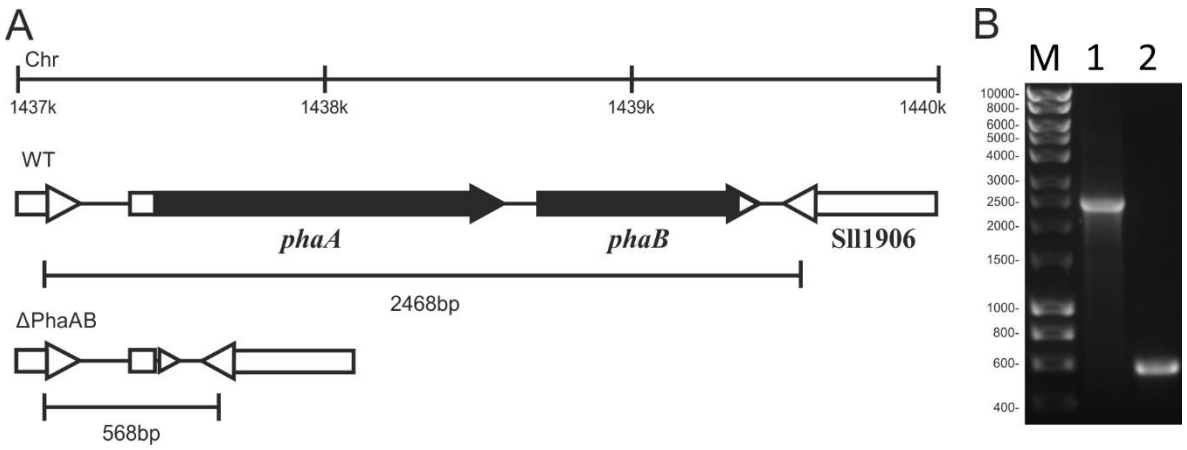

Figure 8. Generation of phaAB unmarked knockout. (a) Schematic representation of locus location in the *Synechocystis* genome (top), and wild-type (middle) and ΔPhaAB (bottom) profile expected. **(b)** Lane 'M', molecular size standards; Lane 1, wild-type + CpcC2PRfor/CpcC2PRrev+myc; Lane 2, ΔPhaAB + CpcC2PRfor/ CpcC2PRrev.

4.2 Optimizing *Synechocystis* culture dilutions by employing a standard curve

Diluting cultures to a precise OD, which is necessary for many forms of characterisation, is time consuming when using standard procedures. To more accurately and quickly dilute *Synechocystis* cultures, a standard curve was generated to make absorbance readings proportional to biomass. Absorbance measures the amount of light absorbed or scattered by cells in a suspension. This is proportional to biomass up until a certain point (depending on the type of cell). Beyond which a greater number of cells do not contribute to the absorbance or scattering, as the cells obstruct each other. It is necessary to take this into account when diluting a concentrated starter culture. The theoretical absorbance, proportional to biomass, of a dense culture can be calculated by diluting the culture to a point where cell obstruction in negligible, taking an absorbance reading, and then dividing that reading by the amount the culture was diluted by. This was carried out in series and the data used to produce a polynomial equation which converts absorbance to a theoretical value, proportional to biomass (Figure 9). This equation was compiled into an excel spreadsheet, alongside five dilution equations to make growth experiment dilution calculator. This is, as far as I am aware, this is the first use of this method in diluting bacterial cultures.

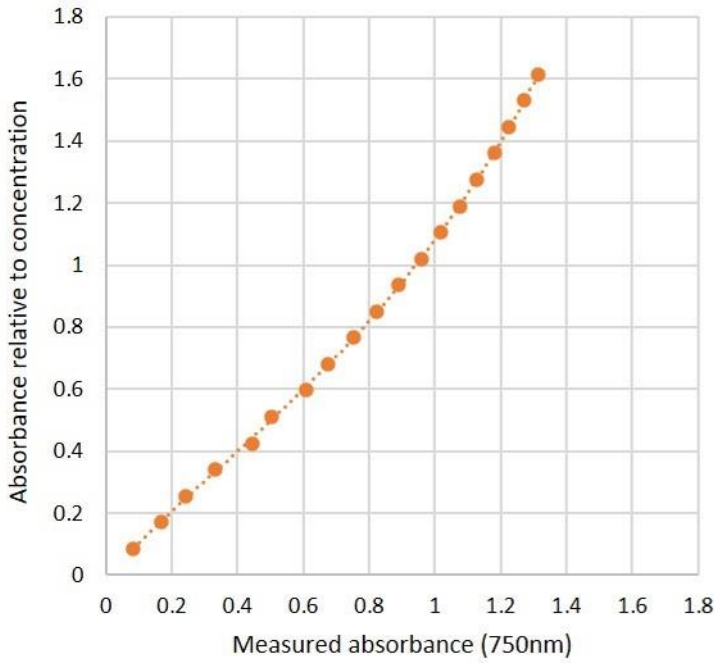

Figure 9. Standard curve to calculate theoretical absorbance value of high-density cultures. Polynomial calibration equation (orange dotted line) is $y = 0.371x^3 – 0.3931x^2 + 1.1039x – 0.0042$.

4.3 PR expressing strains did not show improved growth under green light

In order to determine whether *PR* expression improves growth of *Synechocystis*, strains expressing *PR* were cultured under white light and green light, both at 50 µmol photons m^{-2} s^{-1}. Green light was used to increase the activity PR in contrast to the photosystems and the PBS. The wild-type, ΔPhaAB, Native$_{TS}$PR, PsaF$_{TS}$PR and MscS$_{TS}$PR strains all demonstrated similar growth under both green and white light conditions.

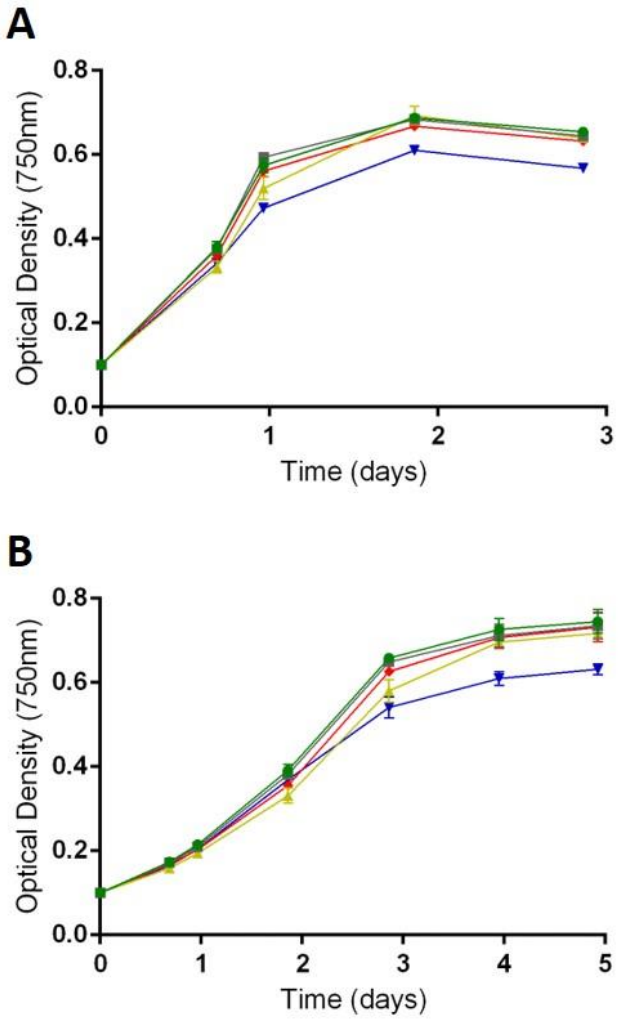

Figure 10. Under both green and white light growth rates are similar between wild-type and PR expressing *Synechocystis* strains, except for MscS$_{TS}$PR which exhibits reduced growth and differences in chlorophyll content. Growth of wild-type (green circles), ΔPhaAB (grey squares), Native$_{TS}$PR (yellow triangles), PsaF$_{TS}$PR (red diamonds) and MscS$_{TS}$PR (up-side down blue triangles). Growth rate under 50 µmol photons m^{-2} s^{-1} of continuous (**a**) green light or (**b**) white light. Error bars indicate standard error of 12 replicates.

4.4 Testing growth of PR expressing strains in larger volume flasks remains inconclusive

In order to confirm that *PR* expression results in increased growth under high light intensity, air bubbling and large culture volume, as observed by Baers *et al.* (Baers *et al.*, manuscript in preparation, strains were cultured thusly. Wild-type, ΔPhaAB and PsaF$_{TS}$PR were cultured under a light intensity of 100 µmol photons m^{-2} s^{-1}, with air bubbling, in a volume of 600 ml. PsaF$_{TS}$PR obtained a higher maximum OD$_{750nm}$ than wild-type by 12.3% and ΔPhaAB by 16.7%. Data points after day 16 are excluded from this calculations as PsaF$_{TS}$PR appeared to be suffering from sulfur starvation (Collier and Grossman, 1992; van Alphen *et al.*, 2018). Further replicates are required to conclusively demonstrate this, which was not possible at this stage of the project.

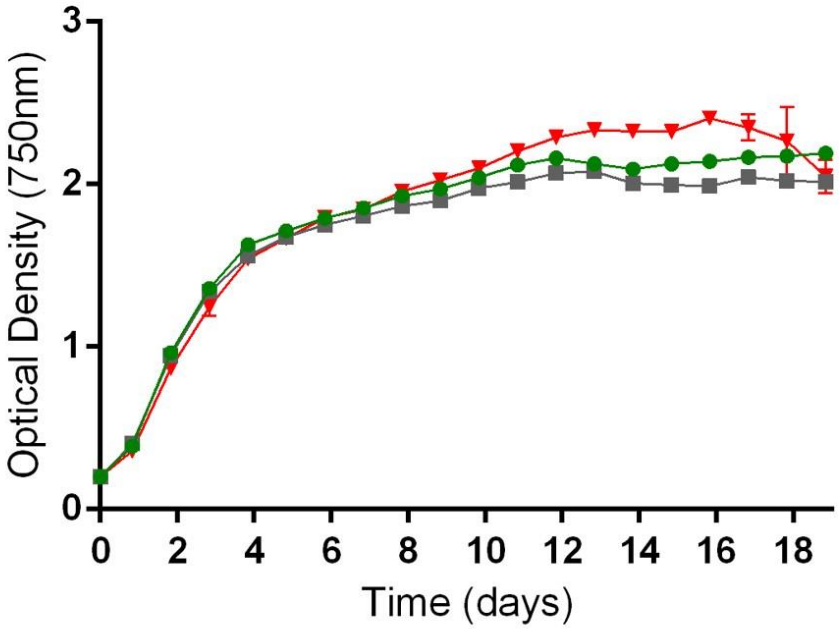

Figure 11. PsaF$_{TS}$PR exhibits increased growth under high light conditions in a large reactor. Growth of wild-type (green circles) (n=1), ΔPhaAB (grey squares) (n=1) and PsaF$_{TS}$PR (upside-down red triangles) (n=2) under continuous high white light (100 µmol photons m^{-2} s^{-1}) + air bubbli ng. Error bars indicate standard error.

4.5 Replacement of phycobilisome genes with PR in the Synechocystis genome

The aim of this section is to replace increasing lengths of the cpc operon with a PR gene (Figure 12). This is to create mutants with varying levels of PBS truncation, alongside PR expression. Plasmids for the marked removal of cpc genes were created in a previous study. Plasmids will be made for the replacement of the *npt1/sacRB* cassette with a PR gene, with or without a C-terminal *myc*-tag.

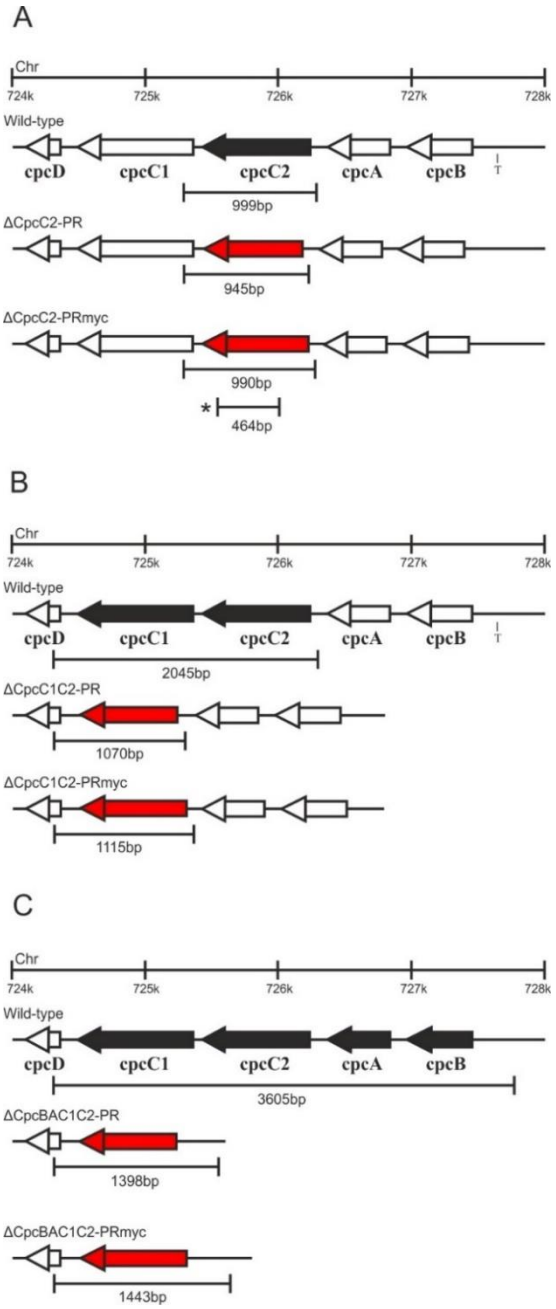

Figure 12. Genetic profiles of planned *Synechocystis* mutant strains. Gene organization of wild-type (top) compared with PR expression (middle) and PR-myc expression (bottom) in **(a)** ΔCpcC2: pcpcT->C, **(b)** ΔCpcC1C2: pcpcT->C and **(c)** Olive strains following amplification with primers flanking the altered sequence or sitting inside the inserted gene (*). Scale is the locus location in the Synechocystis genome. Regions to be deleted in the mutant strains are shaded in black and PR gene is shaded in red. Location of T to C substitution is indicated.

4.5.1 Generation of integrative expression vectors

Plasmids, each containing *PR* with or without a *myc*-tag, and with flanking regions corresponding to different portions of the *cpc* operon, were constructed (Figure 13). The plasmids for generating unmarked mutants were constructed via Gibson Assembly using a protocol by New England Biolabs (Biolabs, 2012). PCR amplifications were carried out on *PR* and plasmids containing antenna gene flanking regions, to produce vectors and inserts respectively, which were verified by gel electrophoresis. Each vector/insert pair was assembled to produce six plasmids. The plasmids each contain the flanking regions of three differing regions of the *cpc* operon surrounding *PR* with or without a *myc*-tag (Figures 14-19). The plasmids were confirmed via an enzyme digest (Figure 20) and verified as correct by DNA sequencing. The different plasmids produced can be used to insert *PR* with or without a C-terminal *myc*-tag into *Synechocystis* genomic DNA, in place of three different regions of the *cpc* operon so that the *PR* is expressed by the native *cpc* promoter and has native start and stop codons.

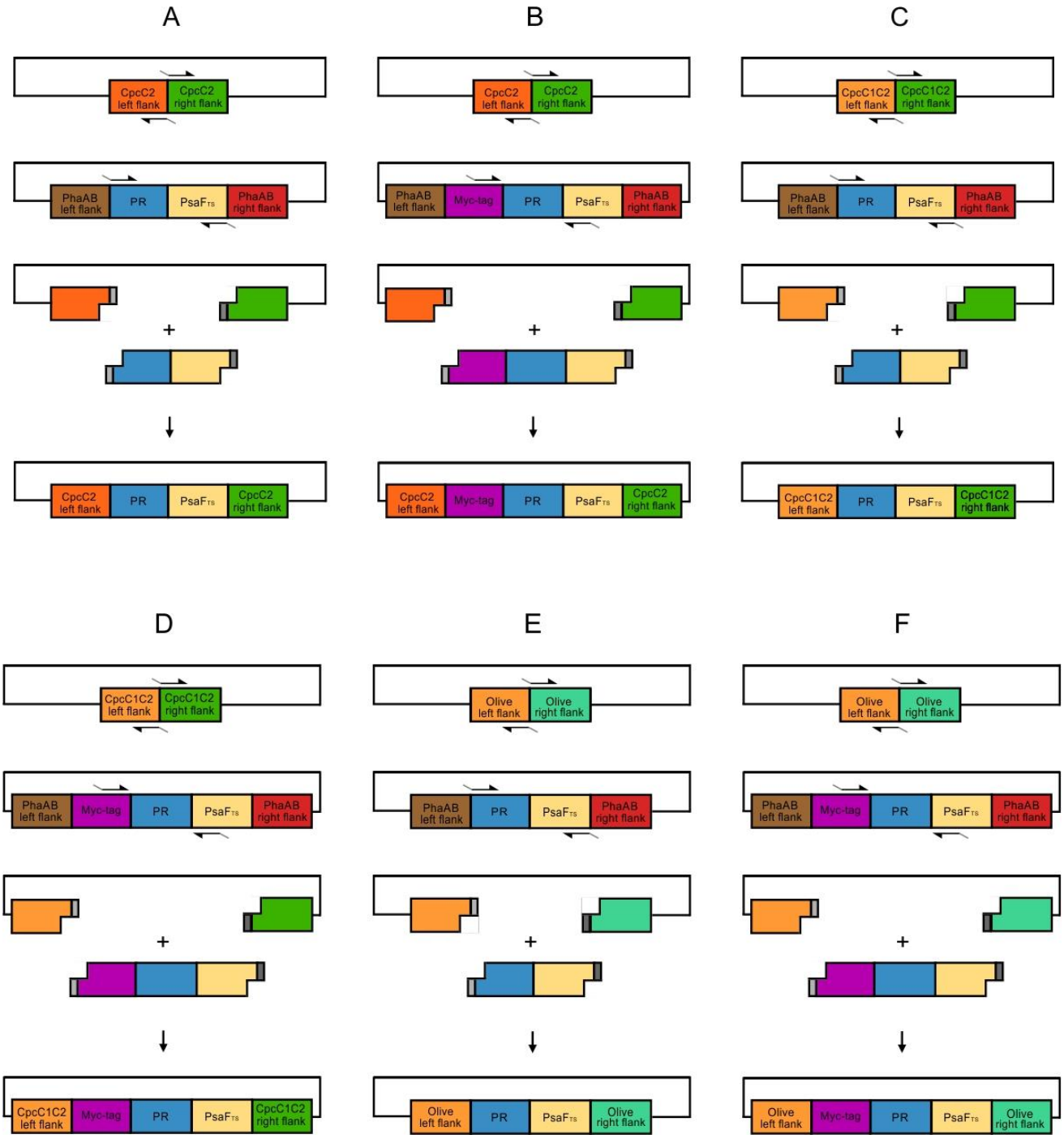

Figure 13. Construction of integrative expression vectors via Gibson Cloning. The Amplification of inserts and vectors, digestion, annealing, extension and ligation to produce plasmids: **(a)** pCpcC2-PR; **(b)** pCpcC2-PR-Myc; **(c)** pCpcC1C2-PR; **(d)** pCpcC1C2-PR-Myc; **(e)** pCpcBAC1C2-PR; **(f)** pCpcCAC1C2-PR-Myc. From top to bottom: amplification of vector; amplification of insert; digestion and annealing; extension.

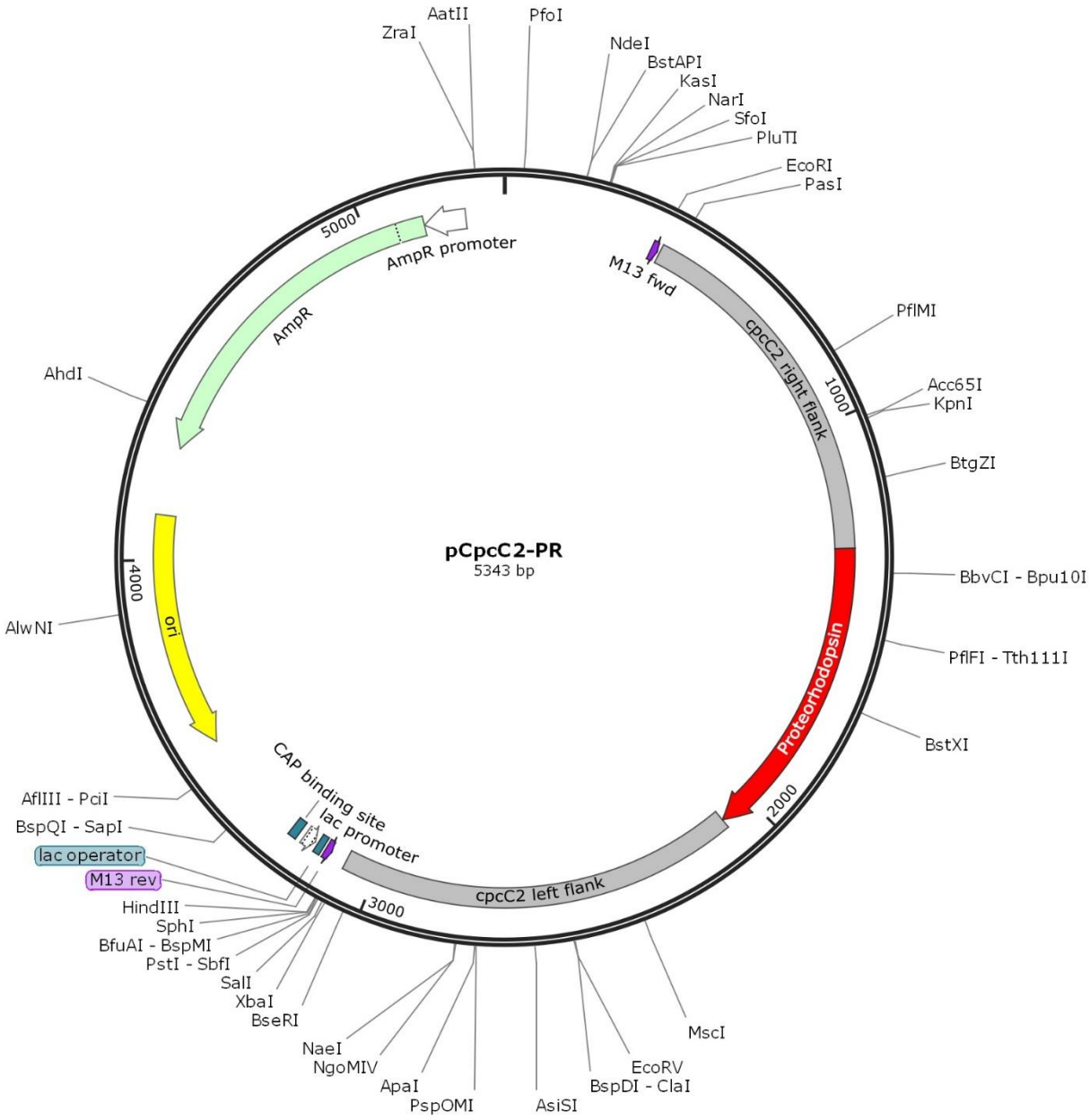

Figure 14. pCpcC2-PR integrative expression vector for *Synechocystis*. The plasmid contains *PR* with an N-terminal *psaF* targeting sequence.

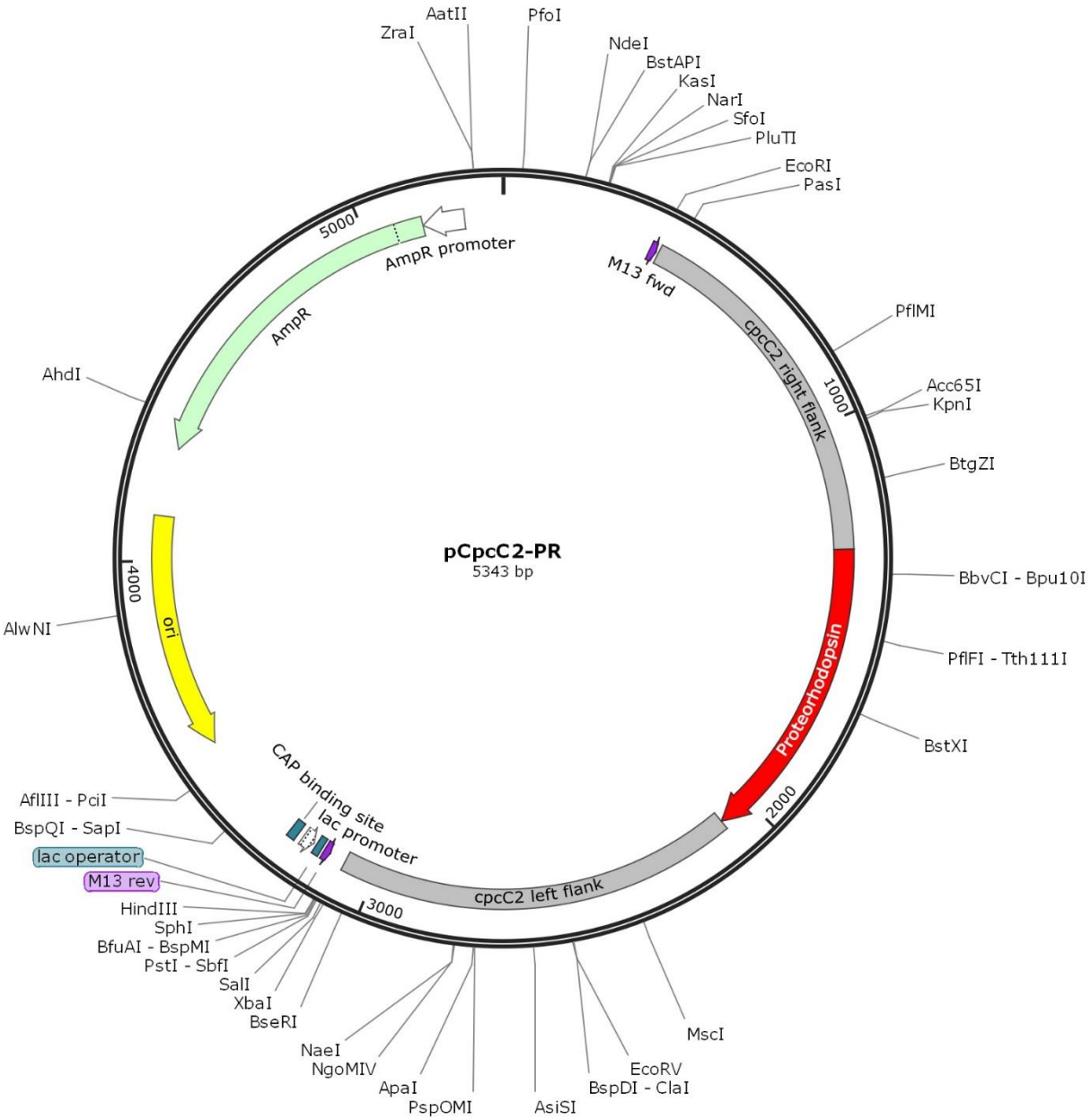

Figure 15. pCpcC2-PR-Myc integrative expression vector for *Synechocystis*. The plasmid contains *PR* with an N-terminal *psaF* targeting sequence and a C-terminal *myc*-tag.

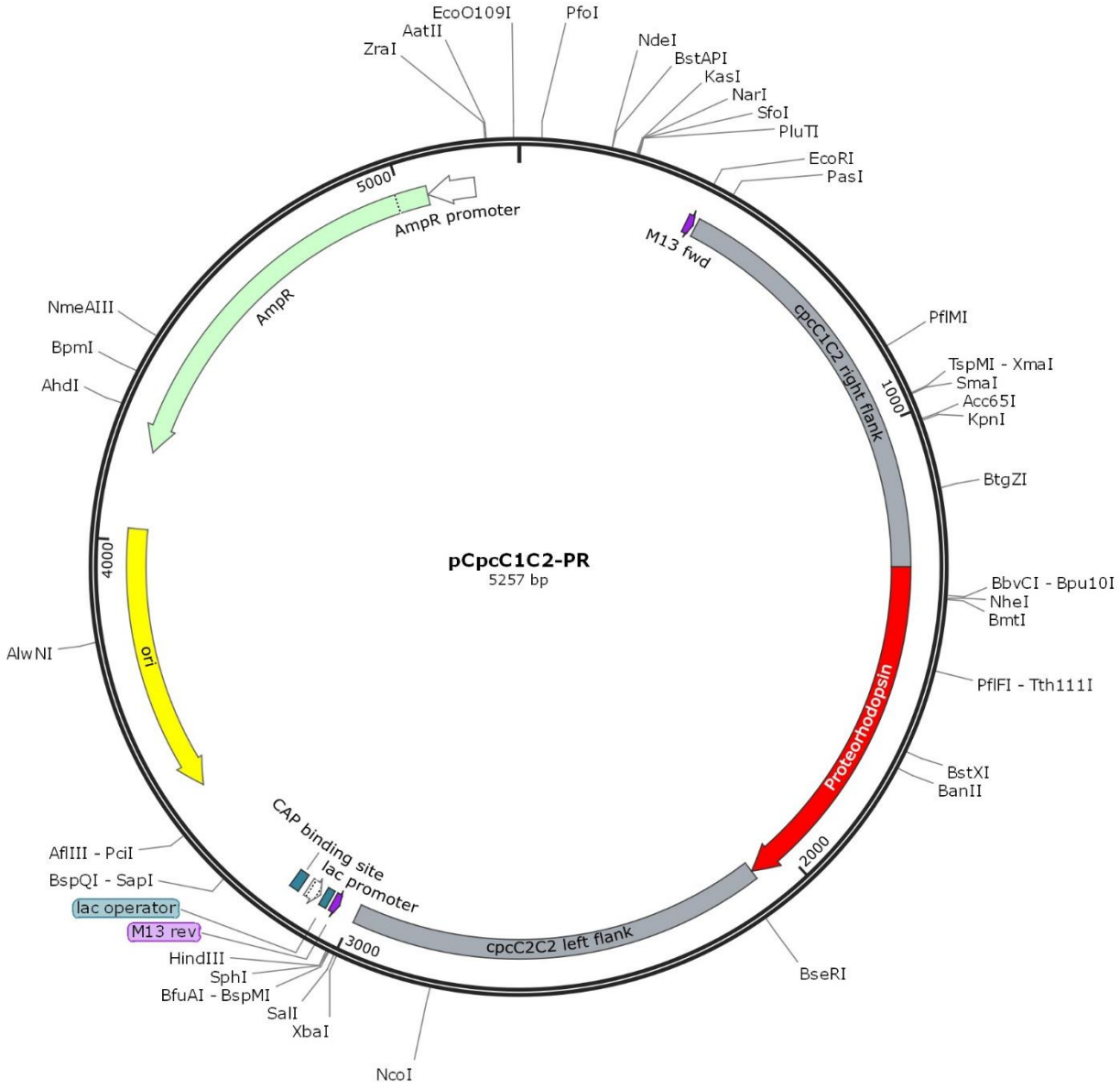

Figure 16. pCpcC1C2-PR integrative expression vector for *Synechocystis*. The plasmid contains PR with an N-terminal *psaF* targeting sequence.

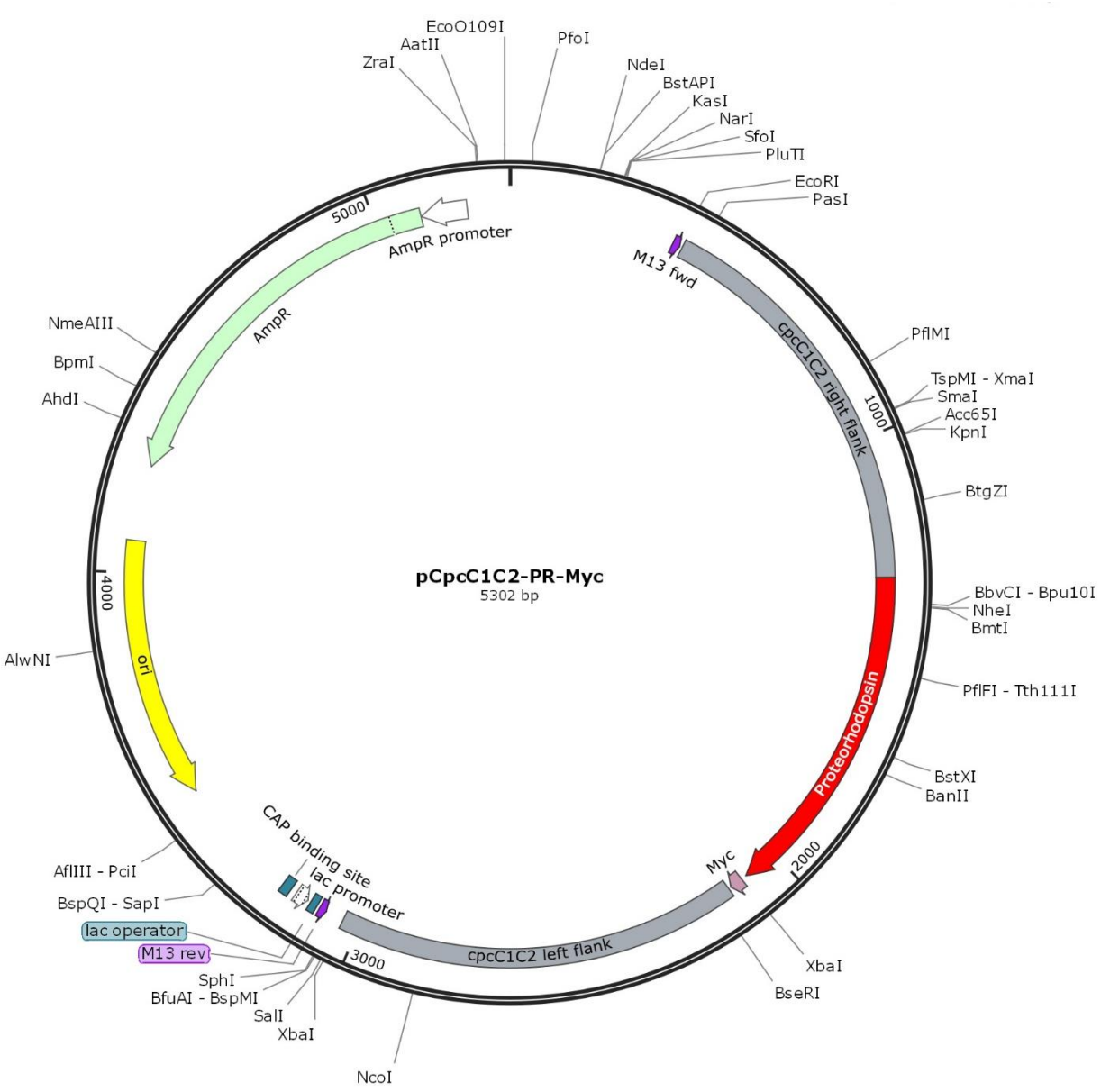

Figure 17. pCpcC1C2-PR-Myc integrative expression vector for *Synechocystis*. The plasmid contains *PR* with an N-terminal *psaF* targeting sequence and a C-terminal *myc*-tag.

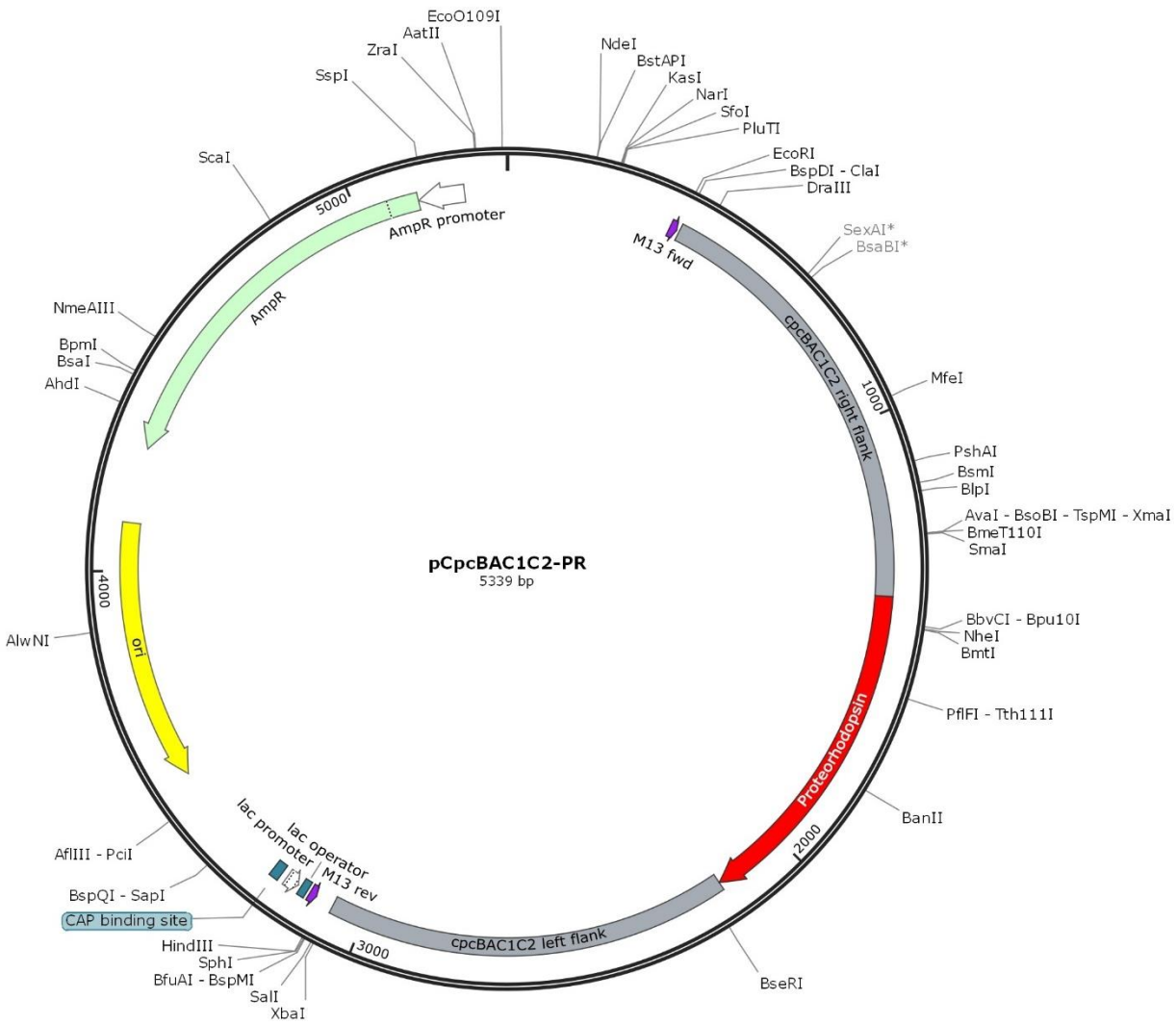

Figure 18. pCpcBAC1C2-PR integrative expression vector for *Synechocystis*. The plasmid contains *PR* with an N-terminal *psaF* targeting sequence.

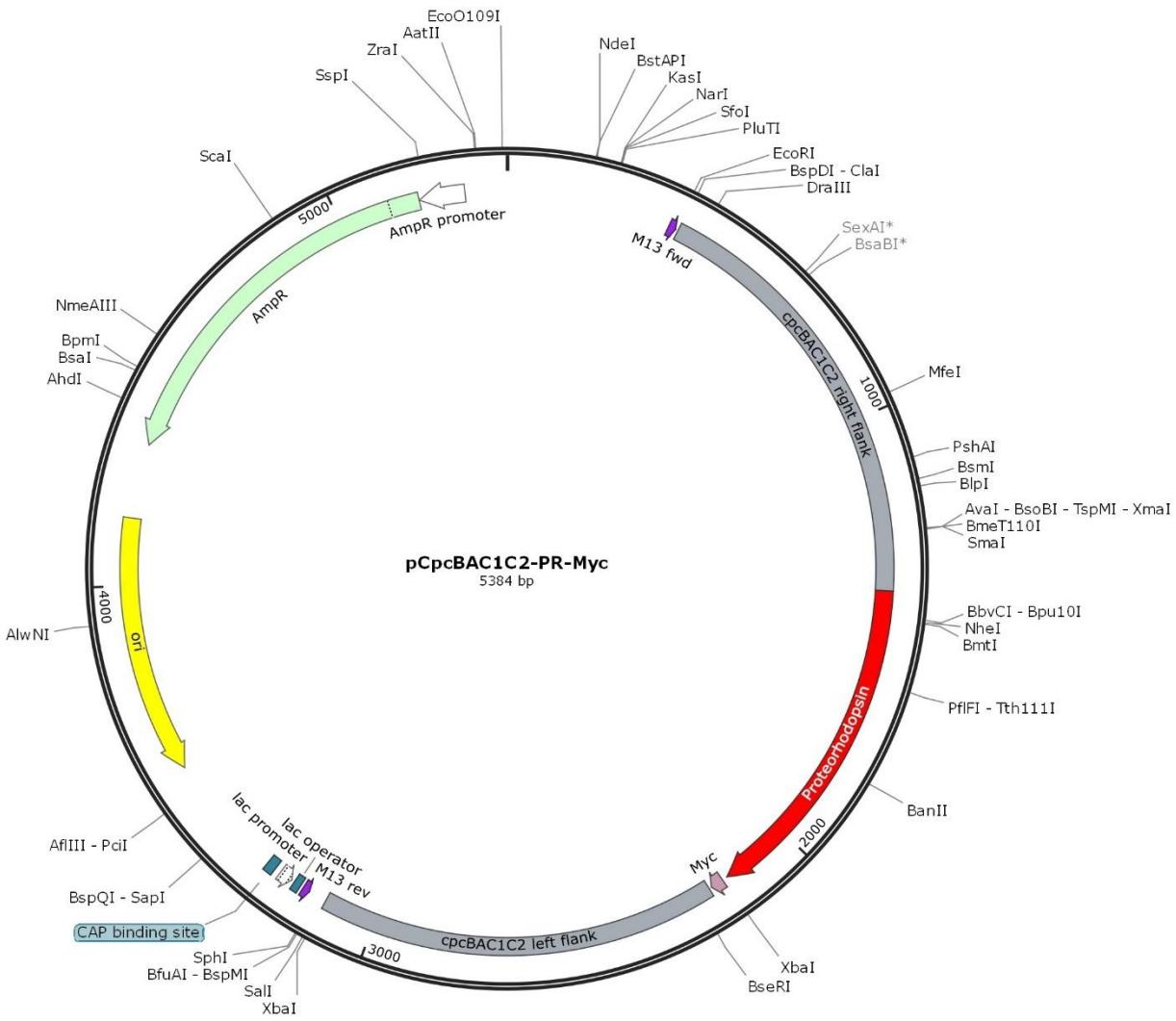

Figure 19. pCpcBAC1C2-PR-Myc integrative expression vector for *Synechocystis*. The plasmid contains *PR* with an N-terminal *psaF* targeting sequence and a C-terminal *myc*-tag.

Figure 20. Plasmids were verified by testing insert sizes following digestion. Each plasmid

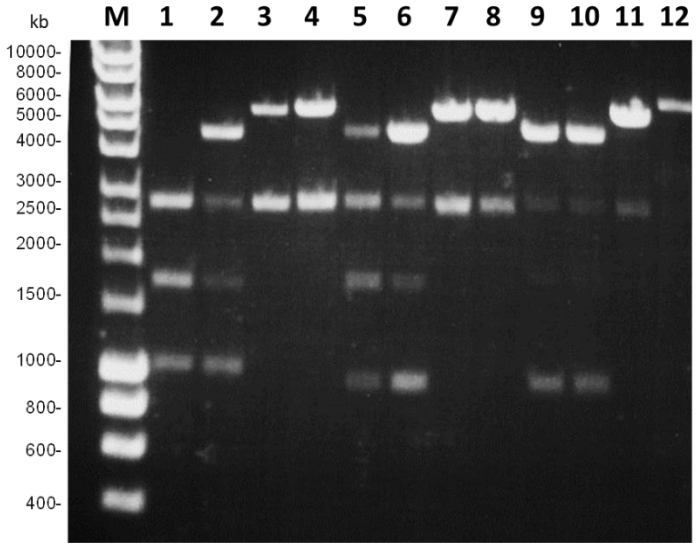

was constructed in duplicate. Plasmids were digested with *Eco*RI and *Bam*HI and the products run on a 1% agarose gel. Expected size of plasmid backbone was 2659 bp. Expected insert sizes are as follows: pCpcC2-PR-Myc (Lanes 1-2), 2729; pCpcC2-PR (Lanes 3-4), 2684; pCpcC1C2-PR-Myc (Lanes 5-6), 2643; pCpcC1C2-PR (Lanes 7-8), 2598; pCpcBAC1C2-PR-Myc (Lanes 9-10), 2725; pCpcBAC1C2-PR (Lanes 11-12), 2680. Inserts containing *myc*-tags were further cleaved into the following sizes: 1692 and 1037 (Lanes 1-2); 1692 and 951 (Lanes 5-6); 1774 and 951 (Lanes 9-10. Lane 'M' contains molecular size standards.

4.5.2 Generation of mutant strains

Unmarked, PR expressing, mutants of *Synechocystis* with two PC hexamers per rod, one PC hexamer per rod, and no PC were constructed by disruption of *cpcC2*, *cpcC1C2*, and *cpcBAC1C2*, respectively, with *PR* with or without a C-terminal *myc*-tag, via a two-step homologous recombination protocol. Marked knockouts were generated by replacing portions of the *cpc* operon with a *npt1*/*sacRB*, using plasmids pCpcC2-2, pCpcC1C2-2 and pCpcBAC1C2-2. Marked knockouts with one or two hexamers of PC per rod were generated from a strain with reduced PC expression, p_{cpc}T->C. Transformed cells were plated and selected for by addition of kanamycin (Lea-Smith, Vasudevan and Howe, 2016). Following complete segregation, markerless constructs containing *PR* (with or without a *myc*-tag) and flanked by the appropriate portions of the *cpc* operon, were introduced. The cells were cultured in the presence of sucrose to select for recombination-mediated replacement of the cassette with the *PR*. Complete segregation was confirmed by PCR assays with primers upstream and downstream of the respective genes (Figure 21). Further validation was carried out by sequencing.

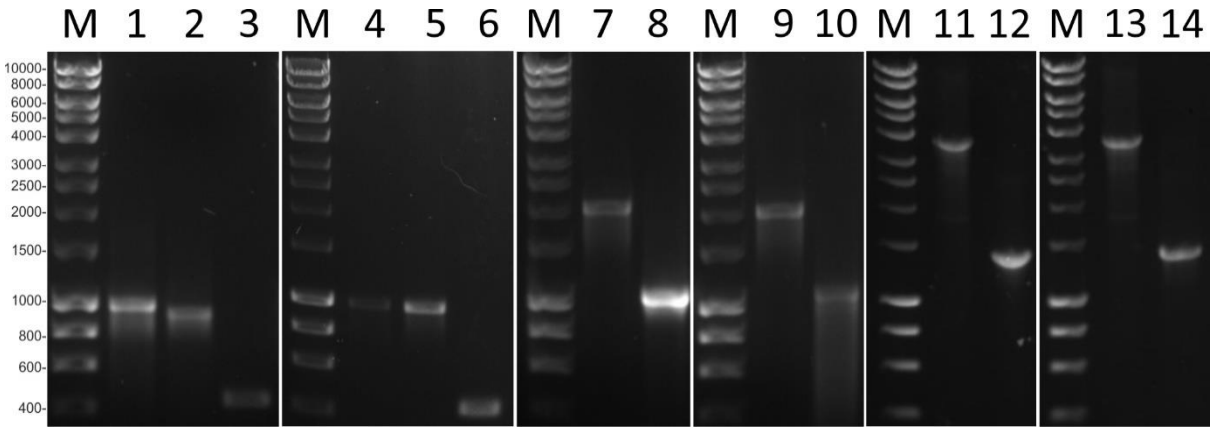

Figure 21. Verification of *Synechocystis* mutant strains. Contents of each lane and expected length of product: Lane 1, wild-type + cpcC2for/cpcC2rev, 999bp; Lane 2, ΔCpcC2: p_{cpc}T->C: $PsaF_{TS}$PR + cpcC2for/cpcC2rev, 945bp; Lane 3, ΔCpcC2: p_{cpc}T->C: $PsaF_{TS}$PR + PRcheckfor/PRcheckrev, 464bp; Lane 4, wild-type + cpcC2for/cpcC2rev, 999bp; Lane 5, ΔCpcC2: p_{cpc}T->C: $PsaF_{TS}$PR-Myc + cpcC2for/cpcC2rev, 990bp; Lane 6, ΔCpcC2: p_{cpc}T->C: $PsaF_{TS}$PR-Myc + PRcheckfor/PRcheckrev, 464bp; Lane 7, wild-type + cpcC1C2for/cpcC2rev, 2045bp; Lane 8, ΔCpcC1C2: p_{cpc}T->C: $PsaF_{TS}$PR + cpcC1C2for/cpcC2rev, 1070bp; Lane 9, wild-type + cpcC1C2for/cpcC2rev, 2045bp; Lane 10, ΔCpcC1C2: p_{cpc}T->C: $PsaF_{TS}$PR-Myc + cpcC1C2for/cpcC2rev, 1115bp; Lane 11, wild-type + cpcC1C2for/cpcOPErev, 3605bp; Lane 12, Olive: $PsaF_{TS}$PR + cpcC1C2for/cpcOPErev, 1398bp; Lane 13, wild-type + cpcC1C2for/cpcOPErev, 3605bp; Lane 14, Olive: $PsaF_{TS}$PR-Myc + cpcC1C2for/cpcOPErev, 1443bp; Lanes marked 'M' contain molecular size standards.

4.6 Absorbance of green light is not substantially increased in PR mutant during logarithmic growth

In order to determine whether *PR* expression alters the light absorption of *Synechocystis*, the absorbance spectra of whole cells of *PR* expressing strains, harvested during logarithmic phase, were analyzed. The strain PsaF$_{TS}$PR exhibited no difference in absorption of light at 520 nm, the λmax of PR, compared to wild-type. The TLA-PR strains, ΔCpcC1C2: p$_{cpc}$T->C: PsaF$_{TS}$PR and Olive: PsaF$_{TS}$PR also exhibited no difference in absorption at 520nm compared to ΔCpcC1C2: p$_{cpc}$T->C and Olive, respectively.

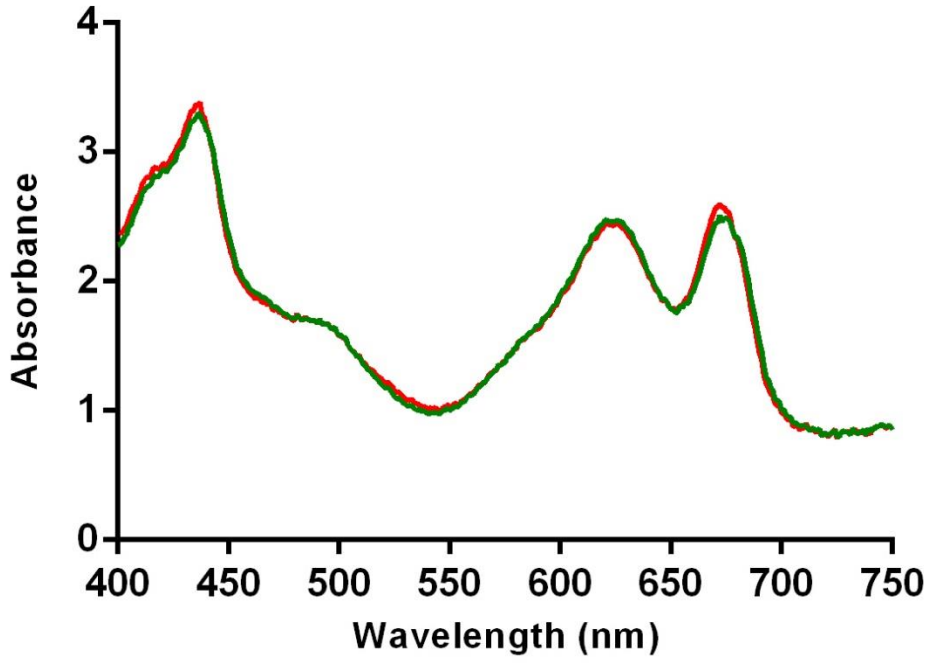

Figure 22. PR expressing strain did not show significantly increased absorbance of light at 520nm during logarithmic growth. Absorbance spectra of wild-type (green) and PsaF$_{TS}$PR (red). Values are averages of three biological replicates and three technical replicates and are standardized to 750 nm.

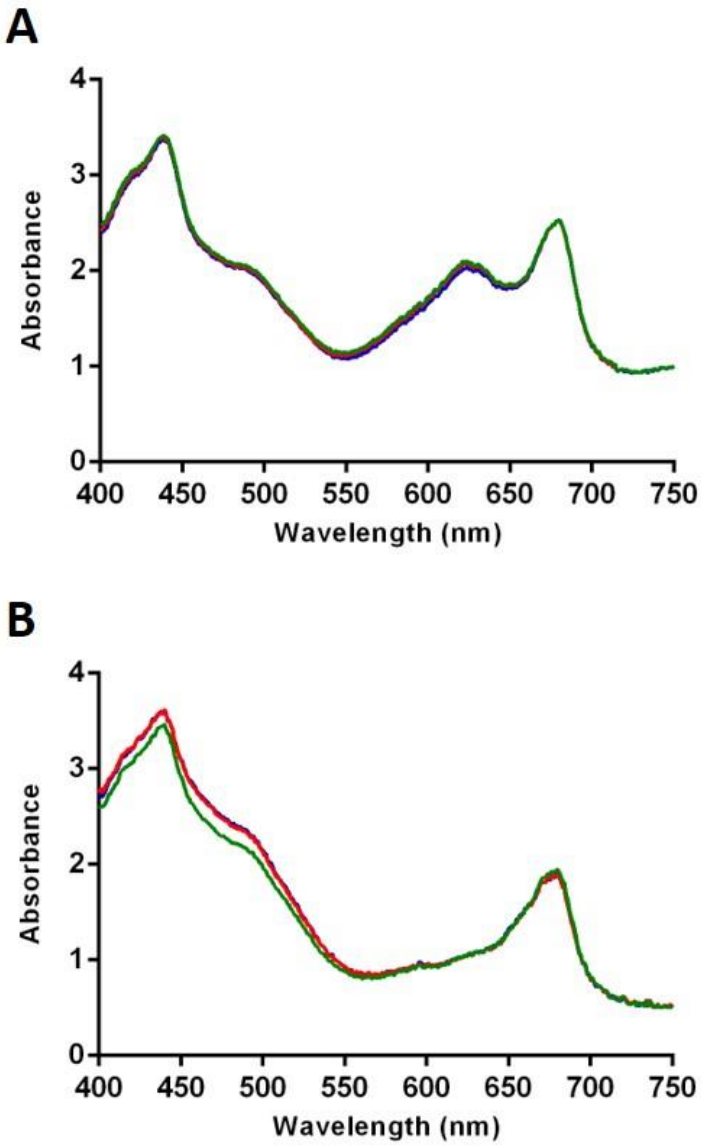

Figure 23. Expression of PR, in strains with two and three removed PC hexamers per rod, did not increase absorbance of light at 520nm during logarithmic growth. Absorbance spectra of TLA (green), TLA-PR (red) and TLA-PR-Myc (blue) strains, with two hexamers removed per rod (**a**) or three hexamers removed per rod (**b**). Values are averages of three biological replicates and three technical replicates and are standardized to 750 nm.

4.7 PR expression increases the photosynthetic rate of the Olive mutant

In order to determine whether photosynthesis and respiration was altered in the engineered strains, an oxygen electrode was employed. Changes in the median oxygen content were measured over periods of increasing light intensity, with intermittent dark periods. The rate of oxygen depletion in the dark periods was added to the rate of oxygen evolution in the light periods to give the gross oxygen production at each light intensity. This generates a light saturation curve. In such curves, the rate of gross oxygen evolution levels off as saturating light intensity is approached, with the maximum rate of photosynthesis designated as Pmax. The strains ΔCpcC2, ΔCpcC1C2, ΔCpcC2: PsaF$_{TS}$PR, ΔCpcC1C2: PsaF$_{TS}$PR, ΔCpcC2: PsaF$_{TS}$PR-Myc and ΔCpcC1C2: PsaF$_{TS}$PR-Myc did not differ significantly in their P_{max} values to wild-type. They did, however, reach Pmax at a higher light intensity, 150 µmol photons m^{-2} s^{-1}, compared to 60 µmol photons m^{-2} s^{-1} for wild-type. The Olive strains reached their Pmax at 350 µmol photons m^{-2} s^{-1}. *PR* expression in the Olive strains had a pronounced effect on the Pmax value. The Pmax of Olive was significantly lower than wild-type, and the Pmax of Olive: PsaF$_{TS}$PR/ Olive: PsaF$_{TS}$PR-Myc was significantly higher than wild-type. Paired Student's *t*-tests ($P<0.05$) were used for statistical analysis.

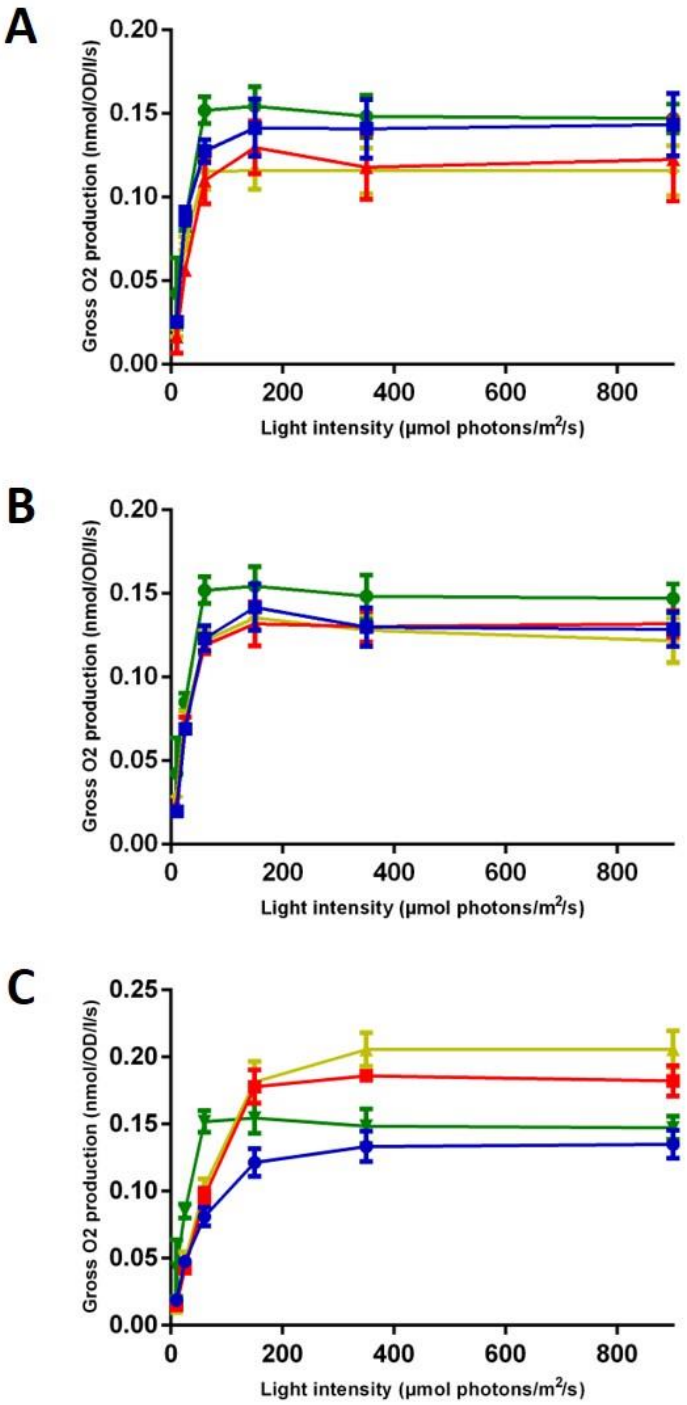

Figure 24. PR expression in the strain Olive significantly increased maximum photosynthetic rate above that of wild-type. Comparison of gross O2 production over a range of light intensities of wild-type (green circles) against TLA (blue squares), TLA-PR (red triangles) and TLA-PR-Myc (yellow diamonds) strains, with two hexamers per rod (a), one hexamer per rod (b) or no hexamers per rod (c). Error bars indicate standard error of between two and five biological replicates.

5 Discussion

A control strain, ΔPhaAB, was generated to confirm whether deletion of the PHB pathway was affecting growth in the strain $PsaF_{TS}PR$. The growth characterisation results of this study, as well as those from Baers *et al.*, implies that PR expression does not improve ATP production during exponential phase but does so during late logarithmic/stationary phase if light remains the limiting factor and if cultures are at high density in larger volumes. Under high light intensity, air bubbling and long pathlength conditions, $PsaF_{TS}PR$ obtained a higher maximum OD_{750nm} than wild-type by 12.3% and ΔPhaAB by 16.7% (Figure 11). This is consistent with the results observed by Baers *et al.* comparing wild-type and $PsaF_{TS}PR$ (Figure 6). Though currently inconclusive without further replicates, the result fits the hypothesis that PR is most effective when other (non-green) wavelengths of visible light are not penetrating dense cultures. However, this study did not observe an increase in logarithmic growth when $PsaF_{TS}PR$ was compared to wild-type under green light (Figure 10). Baer's *et al.*'s green light study required repetition for several reasons. An increase in growth on only days 4 and 6 was observed, which is not sufficient evidence that PR expression increases logarithmic growth and there were also issues with the photobioreactor setup, in that the cells were exposed to small amounts of white light. Our green light study is more conclusive and implies that there is a second reason that increased growth is not observed during exponential phase, other than low cell density. This may be that during exponential phase *Synechocystis* produces significantly less retinal than in other growth phases (Chen, van der Steen, *et al.*, 2018), resulting in a large portion of the PR in these cultures not being bound to retinal.

Absorption spectrophotometry found that *PR* expression did not result in a significant increase in green light absorption by the cell during exponential phase (Figure 22; Figure 23). This means that the quantity of active PR in the cells is lower than would be expected. The molar extinction coefficient of PR is approximately 5 times lower than that of a PC αβ subunit (Béjà *et al.*, 2001; AnaSpec, 2015) and, therefore, an absorption peak, ~5 times smaller the PBS peak, should have been visible. It could be that, due to low levels of retinal in the cells, the peak is small enough to be masked by carotenoid absorbance. This could be investigated by measuring the absorbance of cultures that are showing a difference in growth, during stationary phase when retinal levels are higher. The disparity between the level of PR and retinal in the cells could also be investigated by measuring the absorbance of *PR* expressing cultures with saturating levels of retinal. If this does lead to increased absorption of green light, further studies may set out to increase retinal synthesis (or reduce degradation) in *PR* expressing

strains. However, it is not evident that this low level of green light absorption by the *PR* expressing strains is a disadvantage. It may be allowing green light to penetrate deeper into cultures while still generating a PMF to drive cellular processes, so that higher densities can be reached.

As expected, all the PBS truncated strains required a higher light intensity to reach Pmax (Figure 24), likely due to the cells not being able to absorb as much light. Expressing PR in the PBS truncated strains, with one or two PC hexamers per rod, did not significantly alter their Pmax (Figure 24AB). This suggests that *PR* expression does not affect the rate of photosynthesis. Different groups have theorized that *PR* expression would either increase or decrease the rate of photosynthesis. Chen *et al*. suggested that the increased proton concentration in the thylakoid lumen would inhibit the photosynthetic components (Mullineaux, 2014; Chen, Arents, *et al.*, 2018) via a 'backpressure effect' (Cook *et al.*, 2014). Baers *et al.* suggested that the opposite should occur (Baers *et al.*, manuscript in preparation), specifically that the increased production of ATP would relieve the need for cyclic electron flow. Cyclic electron transport occurs around PSI to further increase the proton gradient when the ATP:NADPH ratio is not optimal for cellular requirements (Lea-Smith *et al.*, 2016). Perhaps these two mechanisms are counteracting each other, or the effect of expressing *PR* on oxygen evolution is too small to be noticeable.

Expression of *PR* in the Olive strain greatly increased the strains Pmax, from a rate significantly lower than wild-type in the Olive strain to a rate significantly higher than wild-type (Figure 24C). This further substantiates the idea that severe reduction of the PBS results in a deleterious widespread upregulation of genes. Here, the expression of *PR* in Olive relieves the excess capacity for protein production, similar to the expression of a resistance marker in the Olive strain generated by Kirst *et al.*, which resulted in the strain not being photosynthetically impaired. However, this does not explain why Olive: PsaF_{TS}PR had an increased Pmax, by 33.2%. Previous studies of Olive mutants have not found that PBS truncation resulted in increased photosynthetic efficiency of individual cells. The reasoning behind increased photosynthetic efficiency of Olive: PsaF_{TS}PR warrants further investigation. Irrespective, this may lead to Olive: PsaF_{TS}PR having an increased growth rate during exponential phase.

The generation of a very promising strain, Olive: PsaF_{TS}PR, is a primary outcome of this work. Characterisation carried out in this study, as well as characterisation of similar mutants in previous studies, suggests that Olive: PsaF_{TS}PR will have several traits which optimise it for

growth under the condition of high light intensity, air bubbling and long pathlength – the condition of a photobioreactor. Characterisation of the growth properties of Olive: PsaF$_{TS}$PR will need to be performed in larger photobioreactors to determine its suitability for biotechnological applications.

References

Ackermann, J. uwe *et al.* (1995) 'Methylobacterium rhodesianum cells tend to double the DNA content under growth limitations and accumulate PHB', *Journal of Biotechnology*, 39(1), pp. 9–20. doi: 10.1016/0168-1656(94)00138-3.

Al-Haj, L. *et al.* (2016) 'Cyanobacteria as Chassis for Industrial Biotechnology: Progress and Prospects', *Life*, 6(4), p. 42. doi: 10.3390/life6040042.

van Alphen, P. *et al.* (2018) 'Increasing the Photoautotrophic Growth Rate of Synechocystis sp. PCC 6803 by Identifying the Limitations of Its Cultivation', *Biotechnology Journal*. doi: 10.1002/biot.201700764.

AnaSpec (2015) *C - PC (C - Phycocyanin)*. Available at: https://www.anaspec.com/products/product.asp?id=48159 (Accessed: 8 May 2020).

Baers, L. L. *et al.* (2019) 'Proteome mapping of a cyanobacterium reveals distinct compartment organization and cell-dispersed metabolism', *Plant Physiology*. doi: 10.1104/pp.19.00897.

Beckmann, J. *et al.* (2009) 'Improvement of light to biomass conversion by de-regulation of light-harvesting protein translation in Chlamydomonas reinhardtii', *Journal of Biotechnology*. doi: 10.1016/j.jbiotec.2009.02.015.

Beja, O. *et al.* (2000) 'Bacterial rhodopsin: Evidence for a new type of phototrophy in the sea', *Science*. doi: 10.1126/science.289.5486.1902.

Béjà, O. *et al.* (2001) 'Proteorhodopsin phototrophy in the ocean.', *Nature*, 411(6839), pp. 786–789. doi: 10.1038/35081051.

Berla, B. M. *et al.* (2013) 'Synthetic biology of cyanobacteria: Unique challenges and opportunities', *Frontiers in Microbiology*. doi: 10.3389/fmicb.2013.00246.

Biolabs, N. E. (2012) 'Gibson Assembly Master Mix', *Manual*, pp. 1–16. doi: 10.1073/pnas.88.17.7585.

Cassier-Chauvat, C., Veaudor, T. and Chauvat, F. (2016) 'Comparative genomics of DNA recombination and repair in cyanobacteria: Biotechnological implications', *Frontiers in Microbiology*. doi: 10.3389/fmicb.2016.01809.

Chen, M. and Blankenship, R. E. (2011) 'Expanding the solar spectrum used by

photosynthesis', *Trends in Plant Science*, pp. 427–431. doi: 10.1016/j.tplants.2011.03.011.

Chen, Q. *et al.* (2016) 'Expression of holo-proteorhodopsin in Synechocystis sp. PCC 6803', *Metabolic Engineering*, 35, pp. 83–94. doi: 10.1016/j.ymben.2016.02.001.

Chen, Q., Arents, J., *et al.* (2018) 'Combining retinal-based and chlorophyll-based (oxygenic) photosynthesis: Proteorhodopsin expression increases growth rate and fitness of a ΔPSI strain of Synechocystis sp. PCC6803', *Metabolic Engineering*. doi: 10.1016/j.ymben.2018.11.002.

Chen, Q., van der Steen, J. B., *et al.* (2018) 'Deletion of sll1541 in Synechocystis sp. strain PCC 6803 allows formation of a far-red-shifted holoproteorhodopsin in vivo', *Applied and Environmental Microbiology*. doi: 10.1128/AEM.02435-17.

Choi, A. R. *et al.* (2014) 'Cyanobacterial light-driven proton pump, gloeobacter rhodopsin: Complementarity between rhodopsin-based energy production and photosynthesis', *PLoS ONE*, 9(10), pp. 1–10. doi: 10.1371/journal.pone.0110643.

Collier, J. L. and Grossman, A. R. (1992) 'Chlorosis induced by nutrient deprivation in Synechococcus sp. strain PCC 7942: not all bleaching is the same.', *Journal of bacteriology*.

Cook, G. M. *et al.* (2014) 'Energetics of Respiration and Oxidative Phosphorylation in Mycobacteria', *Microbiology Spectrum*. doi: 10.1128/microbiolspec.MGM2-0015-2013.

Craig, E. A. and Schlesinger, M. J. (1985) 'The heat shock respons', *Critical Reviews in Biochemistry and Molecular Biology*. doi: 10.3109/10409238509085135.

Dismukes, G. C. *et al.* (2008) 'Aquatic phototrophs: efficient alternatives to land-based crops for biofuels', *Current Opinion in Biotechnology*, pp. 235–240. doi: 10.1016/j.copbio.2008.05.007.

Dubinsky, V. *et al.* (2017) 'Metagenomic analysis reveals unusually high incidence of proteorhodopsin genes in the ultraoligotrophic Eastern Mediterranean Sea', *Environmental Microbiology*. doi: 10.1111/1462-2920.13624.

Ducat, D. C., Way, J. C. and Silver, P. A. (2011) 'Engineering cyanobacteria to generate high-value products', *Trends in Biotechnology*, pp. 95–103. doi: 10.1016/j.tibtech.2010.12.003.

Fasaei, F. *et al.* (2018) 'Techno-economic evaluation of microalgae harvesting and dewatering systems', *Algal Research*. doi: 10.1016/j.algal.2017.11.038.

Fulbright, S. P. *et al.* (2018) ‘Bacterial community changes in an industrial algae production system’, *Algal Research*. doi: 10.1016/j.algal.2017.09.010.

Galloway, J. N. *et al.* (2004) ‘Nitrogen cycles: Past, present, and future’, *Biogeochemistry*. doi: 10.1007/s10533-004-0370-0.

Grigorieva, G. and Shestakov, S. (1982) ‘Transformation in the cyanobacterium Synechocystis sp. 6803’, *FEMS Microbiology Letters*. doi: 10.1111/j.1574-6968.1982.tb08289.x.

Heidorn, T. *et al.* (2011) ‘Synthetic biology in cyanobacteria: Engineering and analyzing novel functions’, *Methods in Enzymology*, 497, pp. 539–579. doi: 10.1016/B978-0-12-385075-100024-X.

Hoffman, J. *et al.* (2017) ‘Techno-economic assessment of open microalgae production systems’, *Algal Research*. doi: 10.1016/j.algal.2017.01.005.

Imashimizu, M. *et al.* (2003) ‘Thymine at -5 Is Crucial for cpc Promoter Activity of Synechocystis sp. Strain PCC 6714’, *Journal of Bacteriology*, 185(21), pp. 6477–6480. doi: 10.1128/JB.185.21.6477-6480.2003.

Kaneko, T. *et al.* (1996) ‘Sequence analysis of the genome of the unicellular cyanobacterium synechocystis sp. strain PCC6803. II. Sequence determination of the entire genome and assignment of potential protein-coding regions’, *DNA Research*, 3(3), pp. 109–136. doi: 10.1093/dnares/3.3.109.

Keasling, J. D. (2010) ‘Manufacturing molecules through metabolic engineering’, *Science*. doi: 10.1126/science.1193990.

Kehoe, D. M. (2010) ‘Chromatic adaptation and the evolution of light color sensing in cyanobacteria’, *Proceedings of the National Academy of Sciences of the United States of America*. doi: 10.1073/pnas.1004510107.

Kirst, H., Formighieri, C. and Melis, A. (2014) ‘Maximizing photosynthetic efficiency and culture productivity in cyanobacteria upon minimizing the phycobilisome light-harvesting antenna size’, *Biochimica et Biophysica Acta - Bioenergetics*, 1837(10), pp. 1653–1664. doi: 10.1016/j.bbabio.2014.07.009.

Kondo, K. *et al.* (2007) ‘The Membrane-Associated CpcG2-Phycobilisome in Synechocystis: A New Photosystem I Antenna’, *PLANT PHYSIOLOGY*, 144(2), pp. 1200–1210. doi:

10.1104/pp.107.099267.

Korotkova, N. and Lidstrom, M. E. (2001) ‘Connection between poly-??-hydroxybutyrate biosynthesis and growth on C1 and C2 compounds in the methylotroph Methylobacterium extorquens AM1’, *Journal of Bacteriology*, 183(3), pp. 1038–1046. doi: 10.1128/JB.183.3.1038-1046.2001.

Kosourov, S. N., Ghirardi, M. L. and Seibert, M. (2011) ‘A truncated antenna mutant of Chlamydomonas reinhardtii can produce more hydrogen than the parental strain’, *International Journal of Hydrogen Energy*. doi: 10.1016/j.ijhydene.2010.10.041.

Kulshreshtha, A. *et al.* (2008) ‘Spirulina in health care management.’, *Current pharmaceutical biotechnology*, 9(5), pp. 400–405. doi: 10.2174/138920108785915111.

Kwon, J. H. *et al.* (2013) ‘Reduced light-harvesting antenna: Consequences on cyanobacterial metabolism and photosynthetic productivity’, *Algal Research*, 2(3), pp. 188–195. doi: 10.1016/j.algal.2013.04.008.

Labarre, J., Chauvat, F. and Thuriaux, P. (1989) ‘Insertional mutagenesis by random cloning of antibiotic resistance genes into the genome of the cyanobacterium Synechocystis strain PCC 6803’, *Journal of Bacteriology*. doi: 10.1128/jb.171.6.3449-3457.1989.

Lea-Smith, D. J. *et al.* (2014) ‘Phycobilisome-Deficient Strains of Synechocystis sp. PCC 6803 Have Reduced Size and Require Carbon-Limiting Conditions to Exhibit Enhanced Productivity’, *PLANT PHYSIOLOGY*, 165(2), pp. 705–714. doi: 10.1104/pp.114.237206.

Lea-Smith, D. J. *et al.* (2016) ‘Photosynthetic, respiratory and extracellular electron transport pathways in cyanobacteria’, *Biochimica et Biophysica Acta - Bioenergetics*, 1857(3), pp. 247–255. doi: 10.1016/j.bbabio.2015.10.007.

Lea-Smith, D. J., Vasudevan, R. and Howe, C. J. (2016) ‘Generation of Marked and Markerless Mutants in Model Cyanobacterial Species’, *Journal of Visualized Experiments*, (111). doi: 10.3791/54001.

Lea-Smith, D. J. and Howe, C. J. (2017) ‘The Use of Cyanobacteria for Biofuel Production’, in *Biofuels and Bioenergy*, pp. 143–155.

Liberton, M. *et al.* (2016) ‘Global Proteomic Analysis Reveals an Exclusive Role of Thylakoid Membranes in Bioenergetics of a Model Cyanobacterium’, *Molecular & Cellular Proteomics*. doi: 10.1074/mcp.m115.057240.

Liberton, M. *et al.* (2017) 'Phycobilisome truncation causes widespread proteome changes in Synechocystis sp. PCC 6803', *PLoS ONE*, 12(3). doi: 10.1371/journal.pone.0173251.

Liu, X., Sheng, J. and Curtiss III, R. (2011) 'Fatty acid production in genetically modified cyanobacteria', *Proceedings of the National Academy of Sciences*. doi: 10.1073/pnas.1103014108.

Martinez, A. *et al.* (2007) 'Proteorhodopsin photosystem gene expression enables photophosphorylation in a heterologous host', *Proc. Natl. Acad. Sci. U S A*, 104(13), pp. 5590–5595. doi: 10.1073/pnas.0611470104.

Mary Leema, J. T. *et al.* (2010) 'High value pigment production from Arthrospira (Spirulina) platensis cultured in seawater', *Bioresource Technology*. doi: 10.1016/j.biortech.2010.06.120.

McFadden, B. A. and Tu, C. C. (1967) 'Regulation of autotrophic and heterotrophic carbon dioxide fixation in Hydrogenomonas facilis.', *Journal of Bacteriology*, 93(3), pp. 886–893.

Melis, A. (2009) 'Solar energy conversion efficiencies in photosynthesis: Minimizing the chlorophyll antennae to maximize efficiency', *Plant Science*, pp. 272–280. doi: 10.1016/j.plantsci.2009.06.005.

Mullineaux, C. W. (1992) 'Excitation energy transfer from phycobilisomes to Photosystem I in a cyanobacterium', *Biochimica et Biophysica Acta (BBA)/Protein Structure and Molecular*. doi: 10.1016/0167-4838(92)90483-T.

Mullineaux, C. W. (2014) 'Electron transport and light-harvesting switches in cyanobacteria', *Frontiers in Plant Science*. doi: 10.3389/fpls.2014.00007.

Mussgnug, J. H. *et al.* (2007) 'Engineering photosynthetic light capture: Impacts on improved solar energy to biomass conversion', *Plant Biotechnology Journal*, 5(6), pp. 802–814. doi: 10.1111/j.1467-7652.2007.00285.x.

Nakajima, Y. and Ueda, R. (1997) 'Improvement of photosynthesis in dense microalgal suspension by reduction of light harvesting pigments', *Journal of Applied Phycology*, 9(6), pp. 503–510. doi: 10.1023/A:1007920025419.

Page, L. E., Liberton, M. and Pakrasi, H. B. (2012) 'Reduction of photoautotrophic productivity in the cyanobacterium Synechocystis sp. strain PCC 6803 by phycobilisome antenna truncation', *Applied and Environmental Microbiology*, pp. 6349–6351. doi: 10.1128/AEM.00499-12.

Perin, G. and Jones, P. R. (2019) ‘Economic feasibility and long-term sustainability criteria on the path to enable a transition from fossil fuels to biofuels’, *Current Opinion in Biotechnology*. doi: 10.1016/j.copbio.2019.04.004.

Peschek, G. A. (1999) ‘Photosynthesis and Respiration of Cyanobacteria’, in *The Phototrophic Prokaryotes*. doi: 10.1007/978-1-4615-4827-0_24.

Pinhassi, J. *et al.* (2016) ‘Marine Bacterial and Archaeal Ion-Pumping Rhodopsins: Genetic Diversity, Physiology, and Ecology’, *Microbiology and Molecular Biology Reviews*. doi: 10.1128/MMBR.00003-16.

Plank, T. and Anderson, L. K. (1995) ‘Heterologous assembly and rescue of stranded phycocyanin subunits by expression of a foreign cpcBA operon in Synechocystis sp. strain 6803’, *Journal of Bacteriology*. doi: 10.1128/jb.177.23.6804-6809.1995.

Polle, J. E. W., Kanakagiri, S.-D. and Melis, A. (2003) ‘tla1, a DNA insertional transformant of the green alga *Chlamydomonas reinhardtii* with a truncated light-harvesting chlorophyll antenna size.’, *Planta*. doi: 10.1007/s00425-002-0968-1.

Qi, F. *et al.* (2013) ‘Construction, characterization and application of molecular tools for metabolic engineering of Synechocystis sp.’, *Biotechnology Letters*. doi: 10.1007/s10529-013-1252-0.

Rexroth, S. *et al.* (2011) ‘The plasma membrane of the cyanobacterium gloeobacter violaceus contains segregated bioenergetic domains’, *Plant Cell*. doi: 10.1105/tpc.111.085779.

Ritchie, R. J. and Larkum, A. W. D. (2012) ‘Modelling photosynthesis in shallow algal production ponds’, *Photosynthetica*, 50(4), pp. 481–500. doi: 10.1007/s11099-012-0076-9.

Schopf, J. W. (2013) ‘The fossil record of cyanobacteria’, in *Ecology of Cyanobacteria II: Their Diversity in Space and Time*. doi: 10.1007/978-94-007-3855-3_2.

Stal, L. J. (1992) ‘Poly(hydroxyalkanoate) in cyanobacteria: an overview’, *FEMS Microbiology Letters*. doi: 10.1016/0378-1097(92)90307-A.

Stanier, R. Y. and Bazine, G. C. (1977) ‘Phototrophic Prokaryotes: The Cyanobacteria’, *Annual Review of Microbiology*. doi: 10.1146/annurev.mi.31.100177.001301.

Tredici, M. R. *et al.* (2016) ‘Techno-economic analysis of microalgal biomass production in a 1-ha Green Wall Panel (GWP®) plant’, *Algal Research*. doi: 10.1016/j.algal.2016.09.005.

Ughy, B. and Ajlani, G. (2004) ‘Phycobilisome rod mutants in Synechocystis sp. strain PCC6803’, *Microbiology*, 150(12), pp. 4147–4156. doi: 10.1099/mic.0.27498-0.

Wang, H. *et al.* (2013) ‘The contamination and control of biological pollutants in mass cultivation of microalgae’, *Bioresource Technology*. doi: 10.1016/j.biortech.2012.10.158.

Waterbury, J. B. (2006) ‘The Cyanobacteria—Isolation, Purification and Identification’, in *The Prokaryotes*. doi: 10.1007/0-387-30744-3_38.

Wijffels, R. H., Kruse, O. and Hellingwerf, K. J. (2013) ‘Potential of industrial biotechnology with cyanobacteria and eukaryotic microalgae’, *Current Opinion in Biotechnology*. doi: 10.1016/j.copbio.2013.04.004.

Williams, J. G. K. (1988) ‘Construction of specific mutations in photosystem II photosynthetic reaction center by genetic engineering methods in *Synechocystis* 6803’, *Methods in Enzymology*, 167, pp. 766–778. doi: 10.1016/0076-6879(88)67088-1.

Xu, H. *et al.* (2004) ‘Multiple deletions of small cab-like proteins in the cyanobacterium Synechocystis sp. PCC 6803. Consequences for pigment biosynthesis and accumulation’, *Journal of Biological Chemistry*, 279(27), pp. 27971–27979. doi: 10.1074/jbc.M403307200.

Xue, Y. and He, Q. (2015) ‘Cyanobacteria as Cell Factories to Produce Plant Secondary Metabolites’, *Frontiers in Bioengineering and Biotechnology*. doi: 10.3389/fbioe.2015.00057.

Zilinskas, B. A. and Greenwald, L. S. (1986) ‘Phycobilisome structure and function’, *Photosynthesis Research*, pp. 7–35. doi: 10.1007/BF00024183.

Zwirglmaier, K. *et al.* (2008) ‘Global phylogeography of marine Synechococcus and Prochlorococcus reveals a distinct partitioning of lineages among oceanic biomes’, *Environmental Microbiology*, 10(1), pp. 147–161. doi: 10.1111/j.1462-2920.2007.01440.x.